

SYMMETRY BREAKING IN A GLOBALLY COUPLED MAP OF FOUR SITES

FANNI M. SÉLLEY¹

ABSTRACT. A system of four globally coupled doubling maps is studied in this paper. It is known that for weak interaction such systems have a unique absolutely continuous invariant measure (acim), but the case of stronger coupling is still unexplored. Similarly as in the case of three coupled sites in [14], we prove the existence of a critical value of the coupling parameter such that for stronger interaction, the system has multiple acims. Our proof has several new ingredients in comparison to the one presented in [14]. We strongly exploit the symmetries of the dynamics in course of the argument. This simplifies the computations considerably, and gives us a precise description of the geometry and symmetry properties of the arising asymmetric invariant sets. Some new phenomena are observed which were not present in the case of three sites: the asymmetric invariant sets arise in areas of the phase space which was transient for weaker coupling. A nontrivial symmetric invariant set emerges, shaped by an underlying centrally symmetric Lorenz map. We state some conjectures on further invariant sets, indicating that unlike in the case of three sites, ergodicity breaks down in many steps, and not all of them are accompanied by symmetry breaking.

1. INTRODUCTION

Coupled map systems are simple models of a finite or infinite network of interacting units, termed sites. The dynamics is given by the composition of the (typically chaotic) individual dynamics and a coupling map representing the characteristics of the interaction. The coupling map usually includes a parameter $0 \leq \varepsilon \leq 1$, representing the strength of interaction.

The analysis of coupled map systems is a quite challenging task. The main interest undoubtedly lies in the emergence of bifurcations: as the strength of interaction is varied, the main features of coupled maps can change dramatically. To give a brief overview of the existing literature, we only cite papers connected closely to our work, for more complete lists see the references in [11], [5], [10] and the collection [4]. Most results concern the case of coupling strength close to zero. In this case of weak coupling, similar phenomena are detectable as in the case of an uncoupled map. For example, the existence of a unique SRB measure, possibly with strong chaotic properties can be proved ([7],[8], [10]). Further results are related to the emergence of contracting directions for values of ε close to 1, resulting in the absence of an absolutely continuous invariant measure ([1], [2], [9],[11]). The results for higher values of the coupling strength can be usually thought of as synchronization in some simple sense. Examples include the individual systems behaving asymptotically identically (see the case of two coupled maps for $\varepsilon > 1/2$

¹DEPARTMENT OF STOCHASTICS, INSTITUTE OF MATHEMATICS, BUDAPEST UNIVERSITY OF TECHNOLOGY AND ECONOMICS, EGRY JÓZSEF U. 1, H-1111 BUDAPEST, HUNGARY AND MTA-BME STOCHASTICS RESEARCH GROUP, BUDAPEST UNIVERSITY OF TECHNOLOGY AND ECONOMICS, EGRY JÓZSEF U. 1, H-1111 BUDAPEST, HUNGARY.

Date: March 18, 2022.

AMS subject classification. 37A25; 37E10; 37G99.

Key words and phrases. coupled map systems, ergodicity breaking, asymmetric invariant sets, piecewise affine maps.

in [14]) or acquiring some more complicated yet fixed formation (three systems acting interdependently on the circle are showed to be able to acquire evenly placed positions asymptotically in [11] for $\varepsilon > 1/2$).

Furthermore, numerical simulations suggest that more complicated phenomena are possible. A particularly interesting one is the emergence of *multiple absolutely continuous invariant measures* (acims) in the case when the system is still fully expanding. Such bifurcations can be interpreted as a deterministic analogue of the phase transitions of Ising models in statistical physics ([3], [6],[12]). The coupling parameter in this case should be relatively high, so that the previously mentioned perturbative results do not apply. Hence these results might be interpreted as complex synchronization phenomena. For example see the case of three coupled maps in [14], where it was shown that ergodic components could be interpreted in terms of the relative positions of the sites.

In this paper we are going to study a system specifically constructed to demonstrate such phenomena, often termed ergodicity breaking. The model, introduced by Koiller and Young in [11], is a globally coupled system of N identical circle maps. By standard results in the literature [10], the map has a unique mixing acim for ε values close to zero. Fernandez [5] indicated by simulations of certain order parameters motivated by the symmetries of this map, that by increasing the value of the coupling parameter, multiple acims emerge. In other words, ergodicity is broken at some critical value of ε .

For a small number of sites, precise results exist. Fernandez showed in [5] that for $N = 2$ ergodicity breaking does not occur. Břant and the present author pointed out later, that even though the unique acim is ergodic in the expanding regime, it ceases to be mixing if $1 - \frac{\sqrt{2}}{2} \leq \varepsilon$ [14]. In the case of $N = 3$, it was shown by Fernandez and independently by Břant and the present author, that due to the appearance of asymmetric invariant sets, ergodicity breaking occurs at the value $\frac{4-\sqrt{10}}{2} \approx 0.42$ of the coupling parameter.

However, for $N > 3$, only numerical simulations suggest ergodicity breaking and no rigorous results have been obtained yet. The existing results for $N = 2$ and $N = 3$ were acquired with the help of elementary, yet careful geometric considerations, requiring a detailed understanding of the dynamics. This paper considers *the case of $N = 4$* in this spirit. The results for $N = 2$ were straightforward consequences of well-known facts about centrally symmetric Lorenz-maps, but for $N = 3$, it was not possible to use known results, a precise geometric understanding of the action of a certain 2-dimensional map was necessary. The case is similar with $N = 4$, but now the geometry is considerably more complicated, since the understanding of a 3-dimensional map is required. B. Fernandez revealed in private communications, that he identified two values of the coupling parameter, $\varepsilon_a \approx 0.39$ and $\varepsilon_b \approx 0.43$, where numerical simulations indicate appearance of multiple asymmetric invariant sets. He also devised an algorithm, which by fixing $\varepsilon > \varepsilon_a$, generates an asymmetric invariant set. This algorithm could act as a base for a *computer assisted proof* for ergodicity breaking. Nevertheless, it leaves us with some questions which an analytic proof could answer. For example, the set generated by the algorithm is difficult to interpret geometrically, and the algorithm does not provide any rigorous results about the symmetry properties of the set. The main goal of this paper is to present an *analytic proof of ergodicity breaking*. Although the result is similar to the one obtained in the $N = 3$ case in [14], we now worked out a more systematic proof which is as simple as possible. In particular, we exploit the symmetries of the system and use simple facts of linear optimization to decrease the amount of calculations as much as possible. This methodological simplification is essential given that the $N = 4$ case is far more complex.

The paper is organized as follows: in Section 2, we familiarize ourselves with the dynamics and apply a change of coordinates introduced in [14], to reduce the analysis of our original 4-dimensional system to the analysis of a piecewise affine self-map of the 3-dimensional torus. We describe the system defined by this map in detail and explore its symmetry group. Section 3 contains our theorem stating that there exists a critical value ε^* such that the system is not ergodic for $\varepsilon^* \leq \varepsilon$. In Section 4 we give the technical details needed to prove our theorem and state some conjectures explicitly. We describe an asymmetric set \mathcal{A} that is invariant for $\varepsilon^* \leq \varepsilon$ and show that it does not break a special abelian subgroup of the symmetry group. From simulations it seems clear that this set is in a part of the phase space which is transient for $1 - \frac{\sqrt{2}}{2} \leq \varepsilon < \varepsilon^*$, so it does not appear as a decomposition of a symmetric invariant set, as the case was in the $N = 3$ case. We further describe a nontrivial symmetric invariant set \mathcal{S} . Our conjectures in this section concern the appearance of further invariant sets. We conjecture that another asymmetric invariant set appears at some value $\varepsilon^{**} > \varepsilon^*$. Furthermore, the set \mathcal{S} breaks up countably many times into new symmetric invariant sets as ε goes to $\frac{1}{2}$. Now the picture that ergodicity breaks down in one step does not seem as likely as it seemed after studying the $N = 3$ case. Since proofs are straightforward and lengthy, they can be found in the Appendix.

2. DEFINITION OF THE DYNAMICS

We are going to consider the system of globally coupled doubling maps as defined by Fernandez in [5]. Let $N > 0$ and $\mathbb{T}^N = (\mathbb{R} \setminus \mathbb{Z})^N$ be the N -dimensional torus. We define $F_{\varepsilon, N} : \mathbb{T}^N \rightarrow \mathbb{T}^N$ as

$$(F_{\varepsilon, N}(x))_i = 2 \left(x_i + \frac{\varepsilon}{N} \sum_{j=1}^N g(x_j - x_i) \right) \quad \text{mod } 1, \quad x = (x_s)_{s=1}^N \in \mathbb{T}^N, i = 1 \dots N, \quad (1)$$

where the function g responsible for the features of the interaction is defined as the lift of

$$g(u) = \begin{cases} 0 & \text{if } u = \pm \frac{1}{2}, \\ u & \text{if } u \in (-\frac{1}{2}, \frac{1}{2}) \end{cases}$$

to \mathbb{R} , see Figure 1 for the graph of this map.

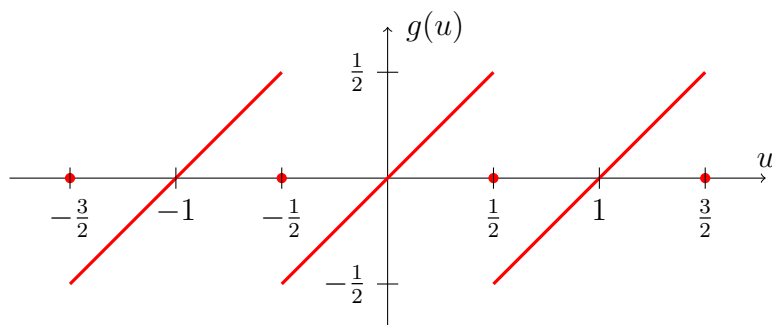


FIGURE 1. The function g .

The map $F_{\varepsilon, N}$ can be regarded as the composition of a mean-field type coupling map

$$(\Phi_{\varepsilon, N}(x))_i = x_i + \frac{\varepsilon}{N} \sum_{j=1}^N g(x_j - x_i) \quad \text{mod } 1, \quad x = (x_s)_{s=1}^N \in \mathbb{T}^N, i = 1 \dots N,$$

and the individual dynamics $T(x) = 2x \pmod 1$, a map well known for its strong chaotic properties.

This dynamical system can be thought of as a model of N interacting particles (usually called *sites* in the coupled map literature) on the circle, changing position according to both the individual dynamics T and the coupling map $\Phi_{\varepsilon,N}$, representing the effect of the other sites. The parameter $\varepsilon \in [0, 1/2)$ is called the coupling parameter, and it controls the strength of the interaction between sites. Specially $\varepsilon = 0$ means no interaction, the position of the sites evolve independently according to T . We only consider values lower than $1/2$ for the coupling parameter, since this is the expanding regime of the map $F_{\varepsilon,N}$ (more precisely, this is the range of the coupling parameter where all of the eigenvalues of the Jacobian of $F_{\varepsilon,N}$ are greater than 1.)

It follows from the abstract framework of [10] that if ε is sufficiently small, this system has a unique absolutely continuous invariant measure. The main goal of our upcoming analysis will be to show that in the case of $N = 4$, this is not true if ε is greater than some critical value, yet still smaller than $1/2$, so that the system is still fully expanding.

From now on we restrict our attention to the special case of four sites. The dynamics of the 4-dimensional system, $F_{\varepsilon,4} : \mathbb{T}^4 \rightarrow \mathbb{T}^4$, takes the form

$$F_{\varepsilon,4}(x_1, x_2, x_3, x_4) = \begin{pmatrix} 2x_1 + \frac{\varepsilon}{2} (g(x_2 - x_1) + g(x_3 - x_1) + g(x_4 - x_1)), \\ 2x_2 + \frac{\varepsilon}{2} (g(x_1 - x_2) + g(x_3 - x_2) + g(x_4 - x_2)), \\ 2x_3 + \frac{\varepsilon}{2} (g(x_1 - x_3) + g(x_2 - x_3) + g(x_4 - x_3)), \\ 2x_4 + \frac{\varepsilon}{2} (g(x_1 - x_4) + g(x_2 - x_4) + g(x_3 - x_4)) \end{pmatrix} \pmod 1.$$

in the coordinates x_1, x_2, x_3 and x_4 .

As in [14], we define the following new coordinates:

$$\begin{aligned} s &= x_1 + x_2 + x_3 + x_4 \pmod 1, \\ p &= x_1 - x_2 \pmod 1, \\ q &= x_2 - x_3 \pmod 1, \\ r &= x_3 - x_4 \pmod 1. \end{aligned}$$

The map $F_{\varepsilon,3}$ is a product of two maps in these new coordinates, namely the first and the last three coordinates evolve independently. More precisely, the map takes the form

$$T \times G_{\varepsilon,3} : \mathbb{T} \times \mathbb{T}^3 \rightarrow \mathbb{T} \times \mathbb{T}^3,$$

such that $G_{\varepsilon,3}$ is the following self-map of \mathbb{T}^3 :

$$G_{\varepsilon,3}(p, q, r) = \begin{pmatrix} 2p + \frac{\varepsilon}{2} (-2g(p) + g(q) + g(q+r) - g(p+q) - g(p+q+r)), \\ 2q + \frac{\varepsilon}{2} (-2g(q) + g(p) + g(r) - g(q+r) - g(p+q)), \\ 2r + \frac{\varepsilon}{2} (-2g(r) + g(q) + g(p+q) - g(q+r) - g(p+q+r)) \end{pmatrix} \pmod 1.$$

It is important to note that $T \times G_{\varepsilon,3}$ is not conjugate to F_ε . We only get a factor of the original system, since the points

$$\left(x_1 + \frac{i}{4}, x_2 + \frac{i}{4}, x_3 + \frac{i}{4}, x_4 + \frac{i}{4} \right), \quad i = 1 \dots 4$$

share the same p, q, r -coordinates. However, detection of ergodicity breaking in a factor implies ergodicity breaking in the original system. Furthermore, ergodicity breaking in the system

$$G_{\varepsilon,3} : \mathbb{T}^3 \rightarrow \mathbb{T}^3$$

implies the lack of ergodicity of the factor, so we are going to continue with the analysis of this system.

$G_{\varepsilon,3}$ is a map of \mathbb{T}^3 , which we are going to represent as the unit cube of \mathbb{R}^3 with opposite faces identified. The map $G_{\varepsilon,3}$ is piecewise affine, and the singularities arise from the singularities of the function g , giving polyhedral domains of continuity. For a complete description of the continuity domains and the form of $G_{\varepsilon,3}$ on them see Appendix A.

In the next subsection we discuss the symmetries of this map.

2.1. Symmetries of the map $G_{\varepsilon,3}$. A symmetry of a map F is a linear transformation S such that

$$S \circ F = F \circ S.$$

The symmetries of the map $F_{\varepsilon,4}$ arise from two sources:

- the inversion symmetry of g and the doubling map (namely that $g(1-u) = 1-g(u)$ and $T(1-u) = 1-T(u)$) implies the inversion symmetry of $F_{\varepsilon,4}$. More precisely,

$$F_{\varepsilon,4} \circ I = I \circ F_{\varepsilon,4},$$

where

$$I : (x_1, x_2, x_3, x_4) \rightarrow (1 - x_1, 1 - x_2, 1 - x_3, 1 - x_4).$$

- every permutation of x_1, x_2, x_3, x_4 is a symmetry of $F_{\varepsilon,4}$:

$$F_{\varepsilon,4} \circ \pi = \pi \circ F_{\varepsilon,4},$$

where π is an element of the fourth order symmetric group (the group of all permutations of four elements).

We note that the symmetry group of the map $F_{\varepsilon,4}$ is generated by the inversion I and a generator of the fourth order symmetric group. An example for the latter is

$$\begin{aligned} \pi_1 &: (x_1, x_2, x_3, x_4) \mapsto (x_2, x_1, x_3, x_4), \\ \pi_2 &: (x_1, x_2, x_3, x_4) \mapsto (x_3, x_2, x_1, x_4), \\ \pi_3 &: (x_1, x_2, x_3, x_4) \mapsto (x_4, x_2, x_3, x_1), \\ \pi_4 &: (x_1, x_2, x_3, x_4) \mapsto (x_1, x_3, x_2, x_4), \\ \pi_5 &: (x_1, x_2, x_3, x_4) \mapsto (x_1, x_4, x_3, x_2), \\ \pi_6 &: (x_1, x_2, x_3, x_4) \mapsto (x_1, x_2, x_4, x_3). \end{aligned}$$

Note that this is not a minimal generator in the sense that for example π_1, π_2 and π_3 already generate the symmetric group. However, we are working with a mean-field model, and no coordinate can have a special role. We constructed a generator with as few elements as possible such that every coordinate has the same role.

These symmetries induce the generators of the symmetry group of $G_{\varepsilon,3}$, which we shall denote by S_G . The inversion of (x_1, x_2, x_3, x_4) induces the inversion of (p, q, r) :

$$S_0 : (p, q, r) \mapsto (1 - p, 1 - q, 1 - r)$$

The permutations induce the following symmetries:

$$\begin{aligned} S_1 : \begin{bmatrix} p \\ q \\ r \end{bmatrix} &\mapsto \begin{bmatrix} -1 & 0 & 0 \\ 1 & 1 & 0 \\ 0 & 0 & 1 \end{bmatrix} \begin{bmatrix} p \\ q \\ r \end{bmatrix} \pmod{1}, \\ S_2 : \begin{bmatrix} p \\ q \\ r \end{bmatrix} &\mapsto \begin{bmatrix} 0 & -1 & 0 \\ -1 & 0 & 0 \\ 1 & 1 & 1 \end{bmatrix} \begin{bmatrix} p \\ q \\ r \end{bmatrix} \pmod{1}, \\ S_3 : \begin{bmatrix} p \\ q \\ r \end{bmatrix} &\mapsto \begin{bmatrix} 0 & -1 & -1 \\ 0 & 1 & 0 \\ -1 & -1 & 0 \end{bmatrix} \begin{bmatrix} p \\ q \\ r \end{bmatrix} \pmod{1}, \\ S_4 : \begin{bmatrix} p \\ q \\ r \end{bmatrix} &\mapsto \begin{bmatrix} 1 & 1 & 0 \\ 0 & -1 & 0 \\ 0 & 1 & 1 \end{bmatrix} \begin{bmatrix} p \\ q \\ r \end{bmatrix} \pmod{1}, \\ S_5 : \begin{bmatrix} p \\ q \\ r \end{bmatrix} &\mapsto \begin{bmatrix} 1 & 1 & 1 \\ 0 & 0 & -1 \\ 0 & -1 & 0 \end{bmatrix} \begin{bmatrix} p \\ q \\ r \end{bmatrix} \pmod{1}, \\ S_6 : \begin{bmatrix} p \\ q \\ r \end{bmatrix} &\mapsto \begin{bmatrix} 1 & 0 & 0 \\ 0 & 1 & 1 \\ 0 & 0 & -1 \end{bmatrix} \begin{bmatrix} p \\ q \\ r \end{bmatrix} \pmod{1}. \end{aligned}$$

Note that

$$\begin{aligned} \pi_4 = \pi_2\pi_1\pi_2 &\Rightarrow S_4 = S_2S_1S_2, \\ \pi_5 = \pi_3\pi_1\pi_3 &\Rightarrow S_5 = S_3S_1S_3, \\ \pi_6 = \pi_3\pi_2\pi_3 &\Rightarrow S_6 = S_3S_2S_3. \end{aligned}$$

We further note two facts: since I commutes with every symmetry of $F_{\varepsilon,4}$, S_0 commutes with every symmetry of $G_{\varepsilon,3}$. Also, each generator symmetry is a \mathbb{Z}_2 -symmetry, applying it twice yields identity.

3. RESULTS

To state the results, we first define the notions of symmetry and invariance we are going to use.

Definition 1. A set $\mathcal{B} \subset \mathbb{T}^3$ is symmetric with respect to the symmetry $S \in S_G$ if $\mathcal{B} = S\mathcal{B}$, and asymmetric with respect to the symmetry $S \in S_G$ if \mathcal{B} and its symmetric image $S\mathcal{B}$ are disjoint.

A set \mathcal{B} is symmetric, if it is symmetric with respect to every element of S_G , and asymmetric if there exists a symmetry in S_G for which \mathcal{B} is asymmetric.

Definition 2. A set $\mathcal{B} \subset \mathbb{T}^3$ is invariant, if $G_{\varepsilon,3}(\mathcal{B}) \subseteq \mathcal{B}$.

Suppose \mathcal{B} is asymmetric with respect to S . If \mathcal{B} is invariant under the dynamics, it is clear that $S\mathcal{B}$ is also invariant, since

$$G_{\varepsilon,3}(\mathcal{B}) \subseteq \mathcal{B} \Rightarrow G_{\varepsilon,3}(S\mathcal{B}) = SG_{\varepsilon,3}(\mathcal{B}) \subseteq S\mathcal{B}.$$

Suppose this set \mathcal{B} is a (not necessarily connected) polyhedral region of \mathbb{R}^3 (this will be the relevant case for us). Of course in this case the symmetric images of \mathcal{B} are also such sets. Using Theorem 1.7 in [15] for these sets independently, we obtain that on each of these sets an absolutely continuous invariant measure is supported.

In conclusion, the existence of such an asymmetric invariant set means that multiple acims exist. Or from another point of view, the acim of maximal support cannot be ergodic.

In our theorem we state that if the value of the coupling parameter is sufficiently high, a set like this exists.

Theorem 1. *There exists an $\varepsilon^* < 1/2$, such that for $\varepsilon^* \leq \varepsilon < 1/2$, there exists an asymmetric invariant set \mathcal{A} of the system $G_{\varepsilon,3} : \mathbb{T}^3 \rightarrow \mathbb{T}^3$.*

The proof of Theorem 1 follows from Proposition 1 of Section 4.2, which includes a precise value of such an ε^* , which is conjectured to be the smallest such value. Proposition 1 also includes the definition of the set \mathcal{A} and a description of its symmetry properties.

At the end of Section 4.2, we state a conjecture that there exists an ε^{**} larger than ε^* , such that if $\varepsilon^{**} \leq \varepsilon$ holds for the coupling parameter, another asymmetric invariant set exists with different symmetry properties than \mathcal{A} . In Conjecture 1, we describe this set in detail, and give a conjecture for the exact value of ε^{**} .

This would indicate that the number of acims not only increases at the value of ε^* , but also at another larger value ε^{**} . In Section 4.3 we formulate a conjecture that countably many further critical values of the coupling parameter exist corresponding to the appearance of new invariant sets, but the new sets are most likely symmetric. These sets are all contained in a special symmetric invariant set, described in Proposition 2. We give a conjecture for the countably many critical values of the coupling parameter in Conjecture 2.

4. INVARIANT SETS

4.1. A centrally symmetric Lorenz map. In this subsection we describe an interval map, which is going to play a central role in the definitions of the invariant sets to be described in this section. Let us define $L_\varepsilon : [\varepsilon/2, 1 - \varepsilon/2] \rightarrow [\varepsilon/2, 1 - \varepsilon/2]$ as

$$L_\varepsilon(v) = \begin{cases} 2(1 - \varepsilon)v + \frac{\varepsilon}{2} & \text{if } \frac{\varepsilon}{2} < v < \frac{1}{2}, \\ 2(1 - \varepsilon)v + \frac{3\varepsilon}{2} - 1 & \text{if } \frac{1}{2} < v < 1 - \frac{\varepsilon}{2}. \end{cases} \quad (2)$$

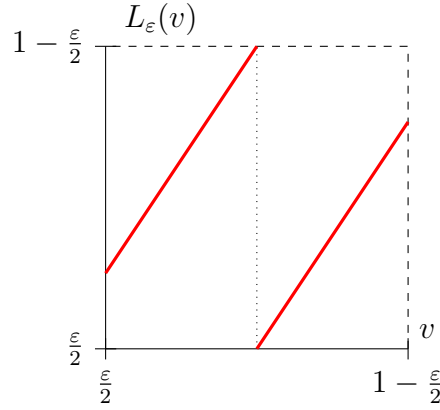
The graph of this map is plotted on Figure 2.

This is a well known centrally symmetric Lorenz map. We are going to state some known facts which will prove useful for us, following the classic work of Parry [13].

For every $0 \leq \varepsilon < 1/2$, the map has an ergodic invariant measure, supported on a finite union of intervals. If $\varepsilon < 1 - \frac{\sqrt{2}}{2}$, the invariant measure is supported on one interval, and it is mixing. For every integer n , when

$$1 - \frac{\sqrt[2^n]{2}}{2} \leq \varepsilon < 1 - \frac{\sqrt[2^{n+1}]{2}}{2},$$

the supporting intervals of the invariant measure can be grouped in 2^n mixing components. By mixing component, we mean a union of intervals, such that $L_\varepsilon^{2^n}$ restricted to it has a mixing invariant measure, and the different components are mapped to each other by L_ε .

FIGURE 2. The graph of L_ε .

For example, take $n = 1$, yielding

$$1 - \frac{\sqrt{2}}{2} \leq \varepsilon < 1 - \frac{\sqrt[4]{2}}{2}.$$

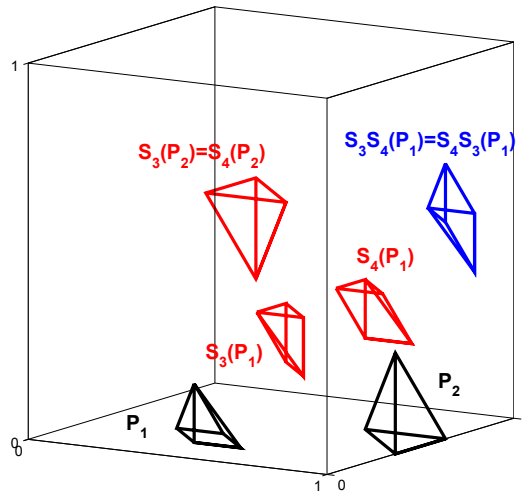
For these values of ε , two mixing components exist:

$$(\varepsilon/2, L_\varepsilon^2(1 - \varepsilon/2)) \cup (L_\varepsilon^2(\varepsilon/2), 1 - \varepsilon/2) \quad \text{and} \quad (L_\varepsilon(\varepsilon/2), L_\varepsilon(1 - \varepsilon/2)). \quad (3)$$

These two components are mapped to each other, and the second iterate of the map restricted to them has a mixing invariant measure. For further details, see Parry [13].

Lastly, we state that the map L_ε has a 2-periodic orbit $p^* \leftrightarrow 1 - p^*$, where

$$p^* = \frac{(1 - \varepsilon)\varepsilon + 3\varepsilon/2 - 1}{1 - 4(1 - \varepsilon)^2} = \frac{\varepsilon - 2}{4\varepsilon - 6}. \quad (4)$$

FIGURE 3. The asymmetric set \mathcal{A} .

4.2. Asymmetric invariant sets. In this section we will give an asymmetric invariant set of the map $G_{\varepsilon,3}$ when $\varepsilon^* \leq \varepsilon < 1/2$. Before defining the set explicitly, we are going to give a few words about our intuition leading to this particular set.

It is a somewhat natural thought that the set should be the union of polyhedra with faces parallel to singularities. Since on certain domains certain coordinates evolve according to L_ε , the constants giving the exact location of the faces will include the period two point p^* of L_ε , defined in terms of ε by equation (4). This will ensure invariance. To ensure asymmetry, the set will be defined to be invariant under a proper subgroup of the symmetry group.

So let us define the following two polyhedra:

	\mathbf{P}_1	\mathbf{P}_2
\mathbf{p}		$p < 1$
\mathbf{q}	$q > \varepsilon/2$	
\mathbf{r}	$r > 0$	$r > 0$
$\mathbf{p} + \mathbf{q}$	$p + q > 1 - p^*$	$p + q > 1 + p^*$
$\mathbf{q} + \mathbf{r}$	$q + r < p^*$	$q + r < 1 - p^*$
$\mathbf{p} + \mathbf{q} + \mathbf{r}$	$p + q + r < 1 - \varepsilon/2$	

Proposition 1. *The set*

$$\mathcal{A} = P_1 \cup P_2 \cup S_3(P_1) \cup S_4(P_1) \cup S_3S_4(P_1) \cup S_3(P_2)$$

is invariant with respect to $G_{\varepsilon,3}$ if

$$0.397 \approx \varepsilon^* = \frac{1}{6} \left(7 - \left(\sqrt[3]{43 + \frac{3\sqrt{177}}{2}} - \sqrt[3]{43 - \frac{3\sqrt{177}}{2}} \right) \right) \leq \varepsilon$$

and it is symmetric with respect to the symmetries S_3 and S_4 , but asymmetric with respect to

$$S_0, S_1, S_2, S_5, \text{ and } S_6.$$

Remark 1. The precise value of ε^* may seem complicated. It is actually the unique real solution of

$$p^* = (1 - \varepsilon)^2, \quad \text{or more explicitly} \quad 4\varepsilon^3 - 14\varepsilon^2 + 15\varepsilon - 4 = 0.$$

Remark 2. By applying the simple facts about the symmetries stated in the last part of Section 2.1, much more information can be deduced from this proposition. In addition to \mathcal{A} , the mutually disjoint sets $S_0(\mathcal{A})$, $S_1(\mathcal{A})$, $S_2(\mathcal{A})$, $S_5(\mathcal{A})$ and $S_6(\mathcal{A})$ are all asymmetric invariant sets. For any element of the symmetry group S_G it can be easily deduced if it is broken by a particular set or not. This can be visualized with a graph, where the vertices are the sets \mathcal{A} , $S_0(\mathcal{A})$, $S_1(\mathcal{A})$, $S_2(\mathcal{A})$, $S_5(\mathcal{A})$ and $S_6(\mathcal{A})$, while the edges indicate the symmetries mapping the set on one end to the set on the other end. By writing an element $S \in S_G$ as $S = S_{i_1} \dots S_{i_j}$, (where $S_{i_k} \in \{S_0 \dots S_6\}$, $k = 1 \dots j$) we get a path from \mathcal{A} following the edges with labels S_{i_k} , $k = 1 \dots j$. If this path ends in \mathcal{A} , the symmetry S is not broken, otherwise it is. The graph is depicted on Figure 4.

It is also an interesting fact, that for any of the asymmetric sets the symmetry subgroup that leaves this set invariant is an abelian subgroup of S_G generated by two symmetries originating from commuting permutations of the original coordinates x_1, x_2, x_3 and x_4 .

The proof of the proposition can be found in Appendix B. Notice that Proposition 1 implies Theorem 1.

We finish this section by stating a conjecture concerning the appearance of further asymmetric invariant sets at some higher value of the coupling parameter.

It is easy to see that faces of the cube are invariant with respect to the dynamics. Explicit calculations of the 2-dimensional dynamics of these subsets show that when

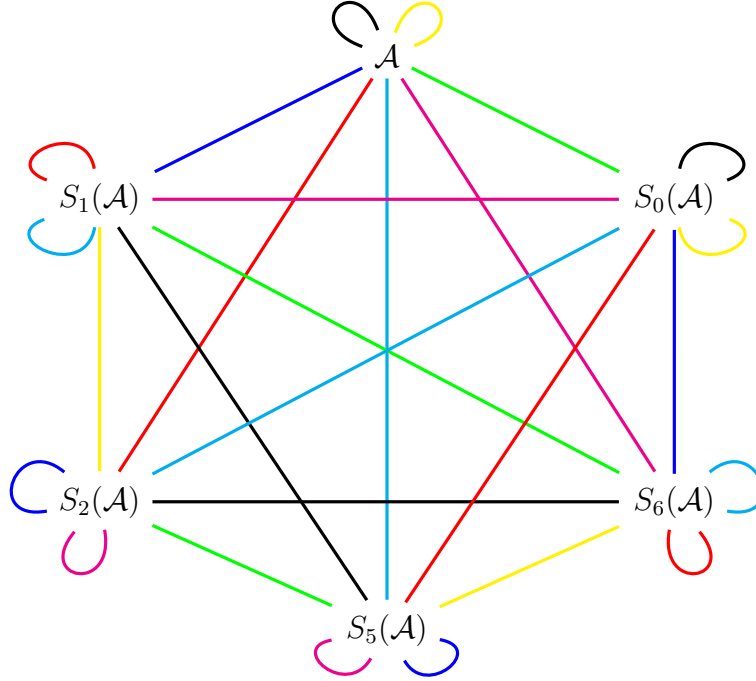


FIGURE 4. Six asymmetric invariant sets and the symmetries connecting them. Edge colors indicate the following symmetries: green – S_0 , blue – S_1 , red – S_2 , black – S_3 , yellow – S_4 , cyan – S_5 , magenta – S_6 .

$$\varepsilon = \frac{5 - \sqrt{17}}{2},$$

new asymmetric invariant sets (polygons) appear.

Regarding the 3-dimensional system, this might mean (by continuity of the dynamics) that positive-Lebesgue measure asymmetric invariant sets also appear at this value of ε . By our simulations it seems likely, that if these polyhedra exist, the previously mentioned polygons are actually the faces of them.

Conjecture 1. *There exists a polyhedron P_3 , such that*

$$\mathcal{A}_2 = P_3 \cup S_1(P_3) \cup S_2(P_3) \cup S_4(P_3) \cup S_2S_1(P_3) \cup S_1S_2(P_3)$$

is symmetric with respect to S_1, S_2 and S_4 , asymmetric with respect to S_0, S_3, S_5 and S_6 , and invariant if

$$0.438 \approx \frac{5 - \sqrt{17}}{2} = \varepsilon^{**} \leq \varepsilon.$$

Remark 3. Notice that the symmetry subgroup leaving \mathcal{A}_2 invariant is generated by S_1 and S_2 , which correspond to the permutations of the original coordinates (x_1, x_2, x_3, x_4) such that x_4 is fixed. In conclusion, the symmetry subgroups leaving the symmetric images of \mathcal{A}_2 invariant also correspond to permutation, which leave one of the coordinates x_1, x_2, x_3 or x_4 fixed.

Remark 4. The conjecture would imply the existence of 7 further asymmetric invariant sets the relations of which are implied by the structure of the symmetry group, as can be seen on the graph on Figure 5.

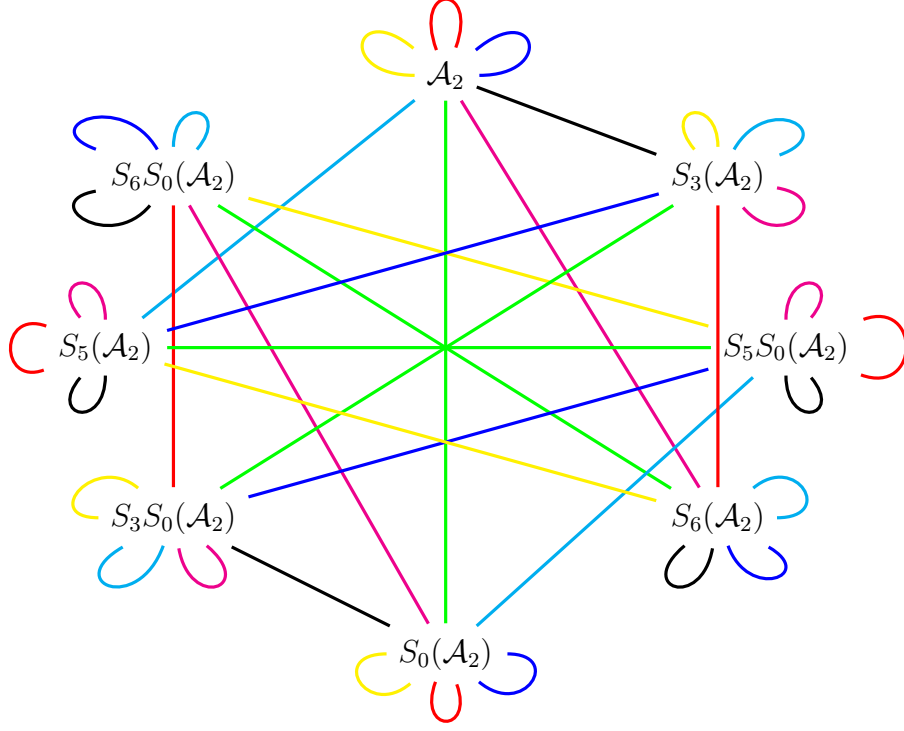


FIGURE 5. Eight conjectured asymmetric invariant sets and the symmetries connecting them. Edge colors indicate the following symmetries: green – S_0 , blue – S_1 , red – S_2 , black – S_3 , yellow – S_4 , cyan – S_5 , magenta – S_6 .

We note that if a description of P_3 could be obtained, the proof of the Conjecture 1 could be completed easily.

4.3. A non-trivial symmetric invariant set. In this section, we are going to define a symmetric invariant set, that is connected to Conjecture 2, stated below.

The intuition leading to this set can be summarized as follows: we define this set as the union of all symmetric images of a certain polyhedron, with faces parallel to singularities. To ensure invariance, we choose the exact locations of these faces with the help of the intervals that support the invariant measure of the map L_ε , when $1 - \frac{\sqrt{2}}{2} \leq \varepsilon < 1 - \frac{\sqrt{2}}{2}$, defined in equation (3). To ensure symmetry, we construct the set as the union of a polyhedron P_0 and all of its symmetric images under the elements of S_G .

Let this polyhedron P_0 be defined as follows:

	\mathbf{P}_0
\mathbf{p}	$L_\varepsilon(\varepsilon/2) < p < L_\varepsilon(1 - \varepsilon/2)$
\mathbf{q}	$\varepsilon/2 < q < L_\varepsilon^2(1 - \varepsilon/2)$
\mathbf{r}	$L_\varepsilon(\varepsilon/2) < r < L_\varepsilon(1 - \varepsilon/2)$
$\mathbf{p} + \mathbf{q} + \mathbf{r}$	$1 + \varepsilon/2 < p + q + r < 1 + L_\varepsilon^2(1 - \varepsilon/2)$

Proposition 2. *The set*

$$\mathcal{S} = P_0 \cup S_0(P_0) \cup S_1(P_0) \cup S_2(P_0) \cup S_3(P_0) \cup S_4(P_0) \cup S_5(P_0) \\ S_0S_1(P_0) \cup S_2S_1(P_0) \cup S_3S_1(P_0) \cup S_4S_1(P_0) \cup S_5S_1(P_0)$$

is symmetric and it is invariant with respect to $G_{\varepsilon,3}$ if

$$1 - \frac{\sqrt{2}}{2} \leq \varepsilon.$$

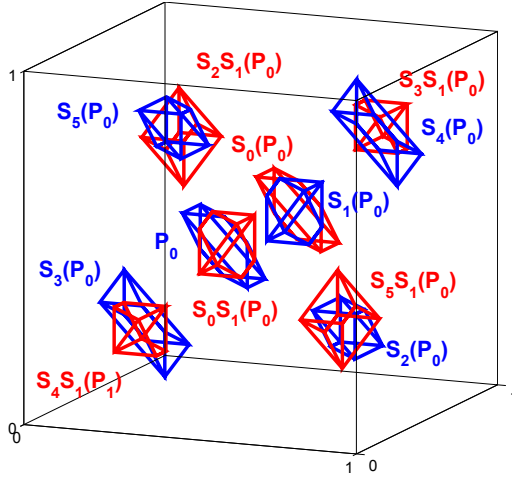


FIGURE 6. The symmetric set \mathcal{S} for $1 - \frac{\sqrt{2}}{2} \leq \varepsilon$.

Remark 5. Provided that $1 - \frac{\sqrt{2}}{2} \leq \varepsilon$, the set \mathcal{S} is the union of 12 convex polyhedra, see Figure 6. The union has 6 disjoint connected components, all of which consist of 2 intersecting convex polyhedra:

- component 1 : $P_0 \cup S_0 S_1(P_0)$,
- component 2 : $S_0(P_0) \cup S_1(P_0)$,
- component 3 : $S_2(P_0) \cup S_5 S_1(P_0)$,
- component 4 : $S_3(P_0) \cup S_4 S_1(P_0)$,
- component 5 : $S_4(P_0) \cup S_3 S_1(P_0)$,
- component 6 : $S_5(P_0) \cup S_2 S_1(P_0)$.

The proof of the proposition can be found in Appendix C.

The point of describing this set was to state an interesting conjecture on the possibility of infinitely many values of the coupling parameter, where new invariant sets appear.

We have stated in Section 4.1, that when $\varepsilon = 1 - \frac{\sqrt{2}}{2}$, the invariant measure of L_ε obtains a support consisting of the union of two mixing components. The symmetric set \mathcal{S} , which is defined with the help of these intervals, becomes invariant at the exact same value of ε . The complicated connection between these two phenomena is described in the proof contained in Appendix C.

We have also stated in Section 4.1 that at every

$$\varepsilon_n = 1 - \frac{\sqrt[2^n]{2}}{2},$$

the support of the invariant measure of L_ε becomes the union of twice as many mixing components than previously. This obviously causes some changes in the structure of the set \mathcal{S} .

Suppose we had a three-dimensional system with every coordinate evolving according to L_ε . In a system like this, new (symmetric) invariant sets appear at every ε_n due to the appearance of new mixing components of the coordinate-maps. Now on each component of \mathcal{S} , if we apply a change of coordinates (depending on the component), $G_{\varepsilon,3}$ acts as the

map previously described. But the connection of the two systems is not clear and proved too complicated to explore. However, our simulations indicate that similar phenomena take place.

Conjecture 2. *At every*

$$\varepsilon_n = 1 - \frac{2^n \sqrt{2}}{2} \quad n > 1,$$

new symmetric invariant sets appear. These new invariant sets are contained in \mathcal{S} and they are symmetric.

5. CONCLUDING REMARKS

The goal of this paper was to contribute to the understanding of a globally coupled map with four sites, a special case of the model introduced by Koiller and Young in [11]. In particular, our aim was to show that for high values of the coupling parameter (indicating strong interaction between the sites), asymmetric invariant sets exist. These sets imply that the invariant measure of maximal support, which is well known to be ergodic and mixing for weak coupling, is in fact not ergodic for such strong coupling. This phenomenon was not present for the model with two sites, but the coupling of three sites did produce it. Proving ergodicity breaking for four sites assures us that it is not an artifact of a somewhat low-dimensional system, but there is a possibility of a tendency.

In this paper, we described a value $\varepsilon^* \approx 0.397$, such that for $\varepsilon \geq \varepsilon^*$, multiple asymmetric invariant sets appear. For such values of the coupling parameter, we gave an asymmetric invariant set \mathcal{A} which has a simple geometric structure, namely it is the union of some polyhedra. Finding this set was a highly nontrivial task, a great amount of simulations led to the conjecture of its precise parameters. We showed that this set \mathcal{A} is not fully asymmetric, it is symmetric with respect to a special abelian subgroup of the map's symmetry group, which is generated by two commuting permutation symmetries. Comparison with the numerical results of Fernandez shows that it is very likely that we succeeded in giving the exact value of ε_a , however, it remains to be shown that no asymmetric invariant sets exist for $\varepsilon < \varepsilon^*$.

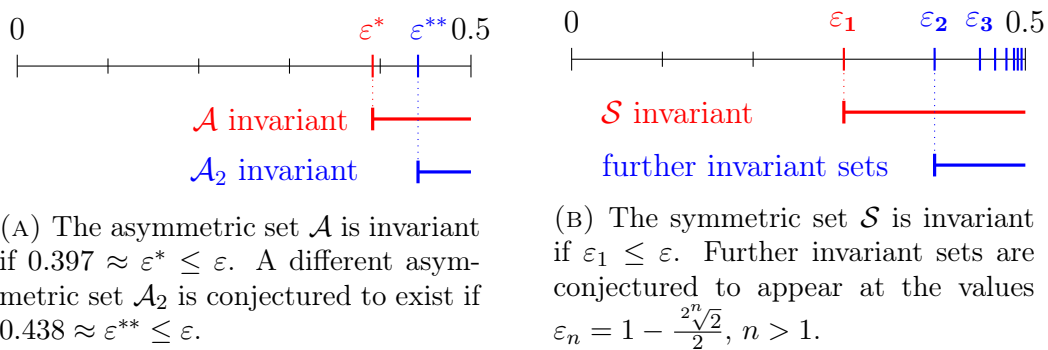


FIGURE 7. Overview of the critical parameters and the corresponding invariant sets. Results are marked with red, conjectures with blue.

Based on explicit calculations on certain lower dimensional invariant subsets of the phase space, we stated a very particular conjecture for the second critical value of the coupling parameter where new asymmetric invariant sets emerge. Our conjectured value is in good agreement with ε_b .

We also described a nontrivial symmetric invariant set \mathcal{S} derived from an underlying one-dimensional Lorenz map. The existence of this set seemed clear from simulating orbits

of random phase points, but finding the right parameters of this set was nontrivial. Based on simulations, we conjecture that new invariant sets arise inside this set for countably many values of the coupling parameter. A better understanding of how the Lorenz map shapes the dynamics of this symmetric invariant set is needed to prove this particularly interesting conjecture.

To summarize, the following picture seems likely: for $\varepsilon_1 = 1 - \sqrt{2}/2$, the attractor is exactly the set \mathcal{S} (for lower values of the coupling parameter it is much larger). When $\varepsilon_1 \leq \varepsilon < \varepsilon^* \approx 0.397$, the attractor is contained in \mathcal{S} . In all of these cases, the system is very likely to be transitive on the attractor. We proved that at the value ε^* the set \mathcal{A} becomes invariant. By straightforward calculations we can obtain that \mathcal{A} and \mathcal{S} are disjoint. Hence new invariant sets emerge in locations where no trajectory returned for $\varepsilon < \varepsilon^*$. At the value of $\varepsilon^{**} \approx 0.438$, similar phenomena can be observed as in the case of ε^* : new asymmetric invariant sets appear in locations left by all trajectories for $\varepsilon < \varepsilon^{**}$. Furthermore, eventually the symmetric invariant set also decomposes into smaller, but still symmetric invariant sets. From these statements some remains to be proved. A summary of the existing results and conjectures is depicted in Figure 7.

We would like to point out that studying this system provided us information on what phenomena seen in the system of three sites was the specialty of that system and what might be more general. By simulations of this system it is clear that *ergodicity does not necessarily break down in one step* (as it happened in the $N = 3$ case), but further invariant sets can emerge for higher values of the coupling parameter than the bifurcation value ε^* (as stated in Conjecture 1.). We have seen that the *asymmetric invariant sets do not necessarily arise as the decomposition of the symmetric invariant set*, as seen in the case of three sites, but they might appear in a part of the phase space which was transient for $1 - \frac{\sqrt{2}}{2} \leq \varepsilon < \varepsilon^*$. A further interesting fact that even in this case, by simulations it seems likely that the symmetric invariant set decomposes into several, although symmetric invariant sets.

Some of the interesting phenomena seen during simulations remained conjectures, so although a proof of ergodicity breaking was obtained, there is possibility for future work even in this particular system.

ACKNOWLEDGEMENTS

The author is grateful for motivating discussions with Bastien Fernandez and Péter Bánt. This work was partially supported by Hungarian National Foundation for Scientific Research (NKFIH OTKA) grant K104745, and Stiftung Aktion Österreich Ungarn (AÖ) grants 87ü6 and 92ü6.

REFERENCES

- [1] C Boldrighini, LA Bunimovich, G Cosimi, S Frigio, and A Pellegrinotti. Ising-type transitions in coupled map lattices. *Journal of statistical physics*, 80(5-6):1185–1205, 1995.
- [2] C Boldrighini, LA Bunimovich, G Cosimi, S Frigio, and A Pellegrinotti. Ising-type and other transitions in one-dimensional coupled map lattices with sign symmetry. *Journal of Statistical Physics*, 102(5-6):1271–1283, 2001.
- [3] LA Bunimovich and Ya G Sinai. Spacetime chaos in coupled map lattices. *Nonlinearity*, 1(4):491, 1988.
- [4] Jean-René Chazottes and Bastien Fernandez. *Dynamics of coupled map lattices and of related spatially extended systems*, volume 671. Springer Science & Business Media, 2005.
- [5] Bastien Fernandez. Breaking of ergodicity in expanding systems of globally coupled piecewise affine circle maps. *Journal of Statistical Physics*, 154(4):999–1029, 2014.
- [6] G Gielis and RS MacKay. Coupled map lattices with phase transition. *Nonlinearity*, 13(3):867–888, 2000.
- [7] Esa Järvenpää. A SRB-measure for globally coupled circle maps. *Nonlinearity*, 10(6):1435, 1997.
- [8] Miaohua Jiang and Yakov B Pesin. Equilibrium measures for coupled map lattices: Existence, uniqueness and finite-dimensional approximations. *Communications in mathematical physics*, 193(3):675–711, 1998.
- [9] Wolfram Just. Globally coupled maps: phase transitions and synchronization. *Physica D: Nonlinear Phenomena*, 81(4):317–340, 1995.
- [10] Gerhard Keller and Carlangelo Liverani. Uniqueness of the SRB measure for piecewise expanding weakly coupled map lattices in any dimension. *Communications in Mathematical Physics*, 262(1):33–50, 2006.
- [11] José Koiller and Lai-Sang Young. Coupled map networks. *Nonlinearity*, 23(5):1121, 2010.
- [12] Jonathan Miller and David A Huse. Macroscopic equilibrium from microscopic irreversibility in a chaotic coupled-map lattice. *Physical Review E*, 48(4):2528, 1993.
- [13] William Parry. The Lorenz attractor and a related population model. In *Ergodic Theory*, pages 169–187. Springer, 1979.
- [14] Fanni Sélley and Péter Bálint. Mean-field coupling of identical expanding circle maps. *J. Stat. Phys.*, 164(4):858–889, 2016.
- [15] Damien Thomine. A spectral gap for transfer operators of piecewise expanding maps. *arXiv preprint arXiv:1006.2608*, 2010.

APPENDIX A: CONTINUITY DOMAINS OF THE MAP $G_{\varepsilon,3}$

The map $G_{\varepsilon,3}$ is a piecewise affine map self-map of \mathbb{T}^3 (represented as the unit cube of \mathbb{R}^3 , with opposite faces identified), and the singularities arising from the singularities of the function g , are intersections of certain planes with the unit cube. This is pictured on Figure 8.

We are going to fix a notation for the continuity domains of the map $G_{\varepsilon,3}$ for further reference. To give these polyhedra systematically, we decompose the cube to 8 smaller cubes according to the singularities $p = 1/2$, $q = 1/2$ and $r = 1/2$ (pictured in light red on Figure 8). We number each cube, and we further decompose them according to the remaining singularities, marking each final domain with a letter. Geometrically, this is pictured on Figures 9-12. To give a precise description, each polyhedral domain can be characterized with a set of inequalities. The minimal such descriptions are found in the Tables 1-4.

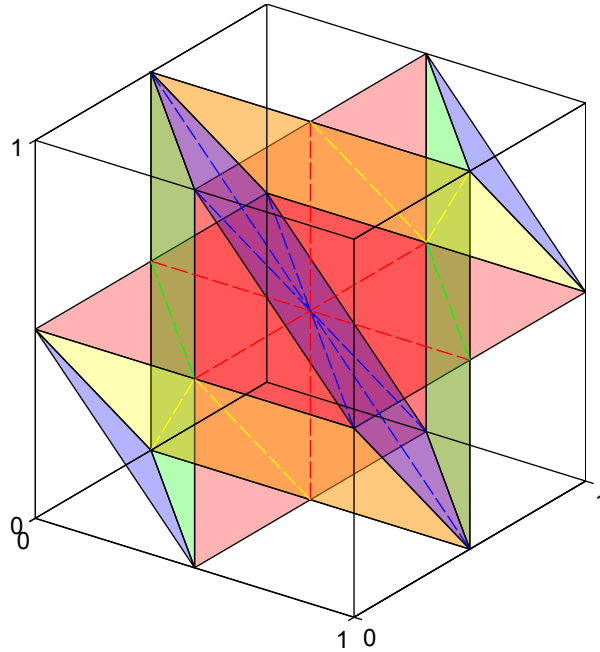


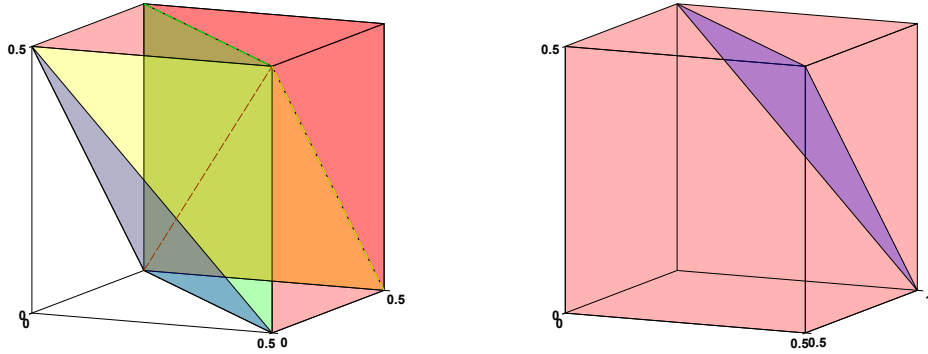
FIGURE 8. Continuity domains of the map $G_{\varepsilon,3}$. \mathbb{T}^3 is represented as the unit cube of \mathbb{R}^3 . The singularities are the intersections of the following planes with the unit cube: $p = 1/2$, $q = 1/2$, $r = 1/2$ (red), $p + q = 1/2$, $p + q = 3/2$ (green), $q + r = 1/2$, $q + r = 3/2$ (yellow), $p + q + r = 1/2$, $p + q + r = 3/2$, $p + q + r = 5/2$ (blue).

As we mentioned, the map $G_{\varepsilon,3}$ is affine on each domain of continuity. More precisely, the linear part is $2(1-\varepsilon)$ times the identity on each domain, and the affine part is a vector (c_1, c_2, c_3) of integers, multiplied by $\varepsilon/2$. More precisely, the image of a point (p, q, r) is

$$\left(2(1-\varepsilon)p + c_1(p, q, r) \frac{\varepsilon}{2}, 2(1-\varepsilon)q + c_2(p, q, r) \frac{\varepsilon}{2}, 2(1-\varepsilon)r + c_3(p, q, r) \frac{\varepsilon}{2} \right) \pmod{1} \quad (5)$$

	p	q	r	p + q	q + r	p + q + r
1a	$p > 0$	$q > 0$	$r > 0$			$p+q+r < 1/2$
1b	$p < 1/2$		$r > 0$	$p+q > 1/2$	$q+r < 1/2$	
1c	$p > 0$		$r < 1/2$	$p+q < 1/2$	$q+r > 1/2$	
1d		$q > 0$		$p+q < 1/2$	$q+r < 1/2$	$p+q+r > 1/2$
1e	$p < 1/2$	$q < 1/2$	$r < 1/2$	$p+q > 1/2$	$q+r > 1/2$	
2a	$0 < p < 1/2$	$1/2 < q < 1$	$0 < r < 1/2$			$p+q+r < 3/2$
2b	$p < 1/2$	$q < 1$	$r < 1/2$			$p+q+r > 3/2$

TABLE 1. Domains of continuity contained in cube 1 and 2.


 (A) Cube 1, where $0 < p, q, r < 1/2$.

 (B) Cube 2, where $0 < p, r < 1/2$ and $1/2 < q < 1$.

FIGURE 9. Cube 1 and 2.

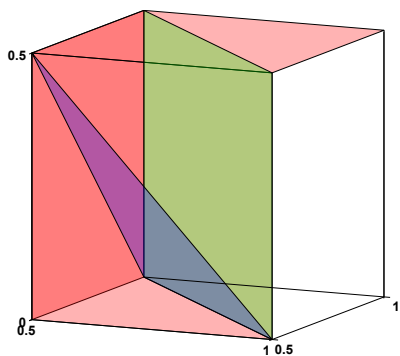
	p	q	r	p + q	q + r	p + q + r
3a	$p > 1/2$	$q > 1/2$	$r < 1/2$	$p+q < 3/2$		$p+q+r > 3/2$
3b	$p > 1/2$	$q > 1/2$	$r > 0$			$p+q+r < 3/2$
3c	$p < 1$	$q < 1$	$0 < r < 1/2$	$p+q > 3/2$		
4a	$1/2 < p < 1$	$q > 0$	$r > 0$		$q+r < 1/2$	
4b	$p > 1/2$	$q < 1/2$	$r < 1/2$		$q+r > 1/2$	$p+q+r < 3/2$
4c	$p < 1$	$q < 1/2$	$r < 1/2$			$p+q+r > 3/2$

TABLE 2. Domains of continuity contained in cube 3 and 4.

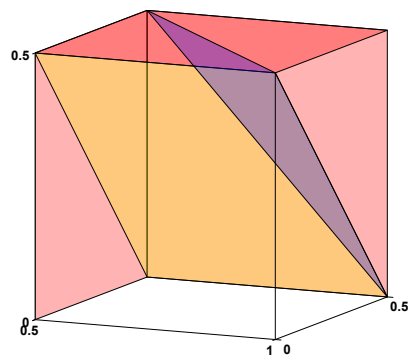
	p	q	r	p + q	q + r	p + q + r
5a	$p > 0$	$q > 0$	$1/2 < r < 1$	$p+q < 1/2$		
5b	$p < 1/2$	$q < 1/2$	$r > 1/2$	$p+q > 1/2$		$p+q+r < 3/2$
5c	$p < 1/2$	$q < 1/2$	$r < 1$			$p+q+r > 3/2$
6a	$p < 1/2$	$q > 1/2$	$r > 1/2$		$q+r < 3/2$	$p+q+r > 3/2$
6b	$p > 0$	$q > 1/2$	$r > 1/2$			$p+q+r < 3/2$
6c	$0 < p < 1/2$	$q < 1$	$r < 1$		$q+r > 3/2$	

TABLE 3. Domains of continuity contained in cube 5 and 6.

on each continuity domain, where c_1, c_2, c_3 take integer values depending only on the continuity domain. The exact values of c_1, c_2 and c_3 on each domain can be found in Table 5.

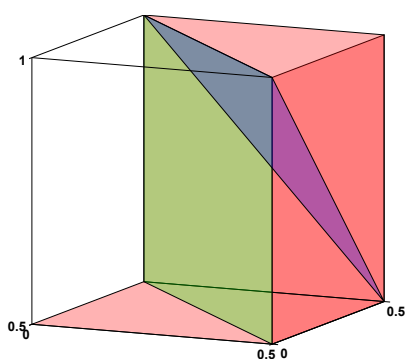


(A) Cube 3, where $0 < r < 1/2$ and $1/2 < p, q < 1$.

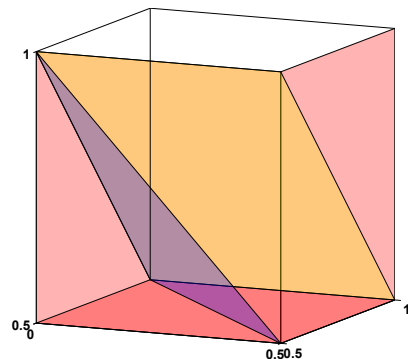


(B) Cube 4, where $0 < q, r < 1/2$ and $1/2 < p < 1$.

FIGURE 10. Cubes 3 and 4.



(A) Cube 5, where $0 < p, q < 1/2$ and $1/2 < r < 1$.

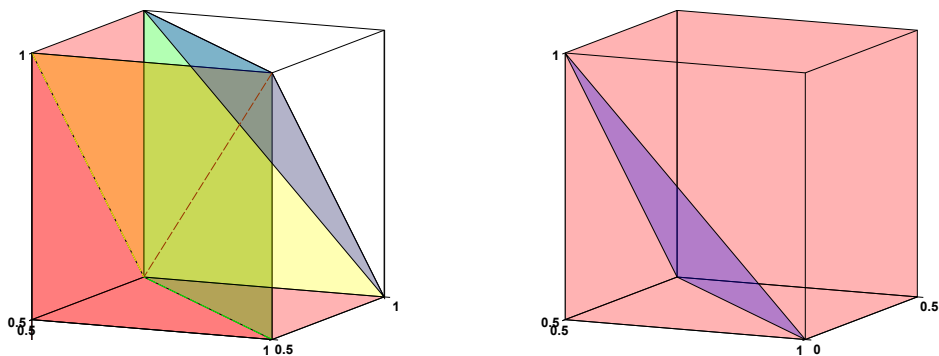


(B) Cube 6, where $0 < p < 1/2$ and $1/2 < q, r < 1$.

FIGURE 11. Cubes 5 and 6.

	\mathbf{p}	\mathbf{q}	\mathbf{r}	$\mathbf{p + q}$	$\mathbf{q + r}$	$\mathbf{p + q + r}$
7a	$p < 1$	$q < 1$	$r < 1$			$p+q+r > 5/2$
7b	$p > 1/2$		$r < 1$	$p+q < 3/2$	$q+r > 3/2$	
7c	$p < 1$		$r > 1/2$	$p+q > 3/2$	$q+r < 3/2$	
7d		$q < 1$		$p+q > 3/2$	$q+r > 3/2$	$p+q+r < 5/2$
7e	$p > 1/2$	$q > 1/2$	$r > 1/2$	$p+q < 3/2$	$q+r < 3/2$	
8a	$1/2 < p < 1$	$0 < q < 1$	$1/2 < r < 1$			$p+q+r > 3/2$
8b	$p > 1/2$	$q > 0$	$r > 1/2$			$p+q+r < 3/2$

TABLE 4. Domains of continuity contained in cube 7 and 8.



(A) Cube 7, where $1/2 < p, q, r < 1$.

(B) Cube 8, where $0 < q < 1/2$ and $1/2 < p, r < 1$.

FIGURE 12. Cubes 7 and 8.

	1a	1b	1c	1d	1e	2a	2b	3a	3b	3c	4a	4b	4c
c_1	0	2	0	1	1	0	1	4	3	2	4	3	4
c_2	0	1	1	0	2	4	4	4	3	3	0	1	1
c_3	0	0	2	1	1	0	1	0	1	0	0	1	2

	5a	5b	5c	6a	6b	6c	7a	7b	7c	7d	7e	8a	8b
c_1	0	1	2	0	1	0	4	2	4	3	3	4	3
c_2	0	1	1	4	3	3	4	3	3	4	2	0	0
c_3	4	3	4	4	3	2	4	4	2	3	3	4	3

TABLE 5. Values of c_1, c_2 and c_3 in Formula 5, according to the continuity domain.

APPENDIX B: PROOF OF PROPOSITION 1

The proof has three parts: we first comment on the symmetry subgroup leaving \mathcal{A} invariant, then prove the dynamical invariance of \mathcal{A} if the condition for ε is met. Lastly, we prove that \mathcal{A} is asymmetric with respect to the symmetries S_0, S_1, S_2, S_5 and S_6 .

Symmetries of \mathcal{A} . We first comment on the statement that \mathcal{A} is symmetric with respect to the symmetries S_3 and S_4 . We will omit the details of the calculations, since they are straightforward and do not have any interesting details.

By simple calculations,

$$\begin{aligned} S_4 S_3(P_1) &= S_3 S_4(P_1), \\ S_4(P_2) &= S_3(P_2), \end{aligned}$$

and by consequence

$$\begin{aligned} S_3 S_4(P_2) &= S_4 S_3(P_2) = P_2, \\ S_3 S_4 S_3(P_1) &= S_4(P_1), \\ S_4 S_3 S_4(P_1) &= S_3(P_1). \end{aligned}$$

(Here equalities should be understood as equalities of sets). So we can see that $S_3(\mathcal{A}) = \mathcal{A}$ and $S_4(\mathcal{A}) = \mathcal{A}$.

Dynamical invariance of \mathcal{A} . We start with an important observation. Suppose $S \in \langle S_3, S_4 \rangle$ and $G_{\varepsilon,3}(P_i) \subset \mathcal{A}$, $i = 1$ or $i = 2$. Then by the definition of symmetry, $G_{\varepsilon,3}(SP_i) = SG_{\varepsilon,3}(P_i) \subset S(\mathcal{A}) \subseteq \mathcal{A}$, since \mathcal{A} is invariant under the symmetry subgroup $\langle S_3, S_4 \rangle$ (as a set). So it is clear that for the dynamical invariance property, we only have to check that $G_{\varepsilon,3}(P_i) \subset \mathcal{A}$ for $i = 1, 2$ once $\varepsilon^* \leq \varepsilon$.

$G_{\varepsilon,3}(P_1) \subseteq \mathcal{A}$. We start by showing that the image of the first polyhedron is a subset of \mathcal{A} , once the condition for ε is met. If $1 - \frac{\sqrt{2}}{2} \leq \varepsilon$, P_1 intersects two continuity domains, $1b$ and $4a$, in the following polyhedra:

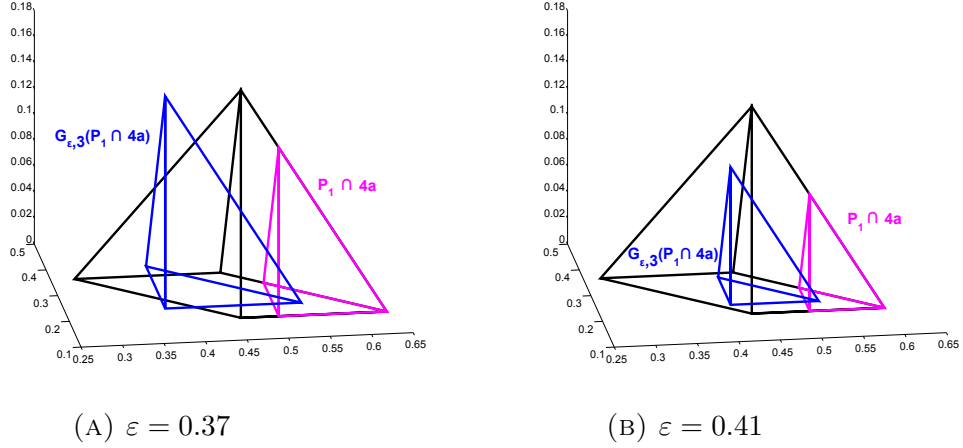
	$\mathbf{P}_1 \cap 1b$	$\mathbf{P}_1 \cap 4a$
\mathbf{p}	$p < 1/2$	$p > 1/2$
\mathbf{q}	$q > \varepsilon/2$	$q > \varepsilon/2$
\mathbf{r}	$r > 0$	$r > 0$
$\mathbf{p} + \mathbf{q}$	$p + q > 1 - p^*$	
$\mathbf{q} + \mathbf{r}$	$q + r < p^*$	
$\mathbf{p} + \mathbf{q} + \mathbf{r}$	$p + q + r < 1 - \varepsilon/2$	$p + q + r < 1 - \varepsilon/2$

By applying the dynamics $G_{\varepsilon,3}$ to these sets, we get the following images:

	$\mathbf{G}_{\varepsilon,3}(\mathbf{P}_1 \cap 1b)$	$\mathbf{G}_{\varepsilon,3}(\mathbf{P}_1 \cap 4a)$
\mathbf{p}	$p < 1$	$p > \varepsilon$
\mathbf{q}	$q > L_\varepsilon(\varepsilon/2)$	$q > L_\varepsilon(\varepsilon/2) - \varepsilon/2$
\mathbf{r}	$r > 0$	$r > 0$
$\mathbf{p} + \mathbf{q}$	$p + q > 1 + p^*$	
$\mathbf{q} + \mathbf{r}$	$q + r < 1 - p^*$	
$\mathbf{p} + \mathbf{q} + \mathbf{r}$	$p + q + r < 2 - L_\varepsilon(\varepsilon/2)$	$p + q + r < 1 - (L_\varepsilon(\varepsilon/2) - \varepsilon/2)$

We immediately see that $G_{\varepsilon,3}(P_1 \cap 1b) \subset P_2 \subset \mathcal{A}$.

$G_{\varepsilon,3}(P_1 \cap 4a) \subset P_1$ holds, if the conditions $p + q > 1 - p^*$ and $q + r < p^*$ hold for the set $G_{\varepsilon,3}(P_1 \cap 4a)$. The infimum of $p + q$ on this set is $L_\varepsilon(\varepsilon/2) + \varepsilon/2$, so for $G_{\varepsilon,3}(P_1 \cap 4a) \subset P_1$ to hold we must have


 FIGURE 13. The image of $P_1 \cap 4a$ for $\varepsilon = 0.37 < \varepsilon^*$ and $\varepsilon = 0.41 > \varepsilon^*$.

$$\begin{aligned}
 L_\varepsilon(\varepsilon/2) + \varepsilon/2 &\geq 1 - p^*, \\
 p^* &\geq (1 - \varepsilon)^2, \\
 \varepsilon &\geq \varepsilon^*.
 \end{aligned}$$

The supremum of $q + r$ on this set is $1 - L_\varepsilon(\varepsilon/2) - \varepsilon/2$, so for $G_{\varepsilon,3}(P_1 \cap 4a) \subset P_1$ to hold we must have

$$\begin{aligned}
 1 - L_\varepsilon(\varepsilon/2) - \varepsilon/2 &\leq p^*, \\
 1 - p^* &\leq L_\varepsilon(\varepsilon/2) + \varepsilon/2, \\
 (1 - \varepsilon)^2 &\leq p^*, \\
 \varepsilon^* &\leq \varepsilon.
 \end{aligned}$$

For an illustration, see Figure 13.

$G_{\varepsilon,3}(P_2) \subseteq \mathcal{A}$. We continue by showing that the image of the second polyhedron is a subset of \mathcal{A} , once the condition for ε is met. P_2 intersects six continuity domains, $3a$, $3b$, $3c$, $4a$, $4b$ and $4c$, in the following way:

	$P_2 \cap 3a$	$P_2 \cap 3b$	$P_2 \cap 3c$
\mathbf{p}	$p < 1$		
\mathbf{q}		$q > 1/2$	$q > 1/2$
\mathbf{r}	$r > 0$		$r > 0$
$\mathbf{p} + \mathbf{q}$	$p + q > 3/2$	$1 + p^* < p + q < 3/2$	$p + q > 1 + p^*$
$\mathbf{q} + \mathbf{r}$	$q + r < 1 - p^*$	$q + r < 1 - p^*$	$q + r < 1 - p^*$
$\mathbf{p} + \mathbf{q} + \mathbf{r}$		$p + q + r > 3/2$	$p + q + r < 3/2$
	$P_2 \cap 4a$	$P_2 \cap 4b$	$P_2 \cap 4c$
\mathbf{p}	$p < 1$		$p < 1$
\mathbf{q}		$q < 1/2$	$q < 1/2$
\mathbf{r}	$r > 0$		
$\mathbf{p} + \mathbf{q}$	$p + q > 1 + p^*$	$p + q > 1 + p^*$	$p + q > 1 + p^*$
$\mathbf{q} + \mathbf{r}$	$q + r < 1/2$	$q + r > 1/2$	$q + r < 1 - p^*$
$\mathbf{p} + \mathbf{q} + \mathbf{r}$		$p + q + r < 3/2$	$p + q + r > 3/2$

By applying the dynamics $G_{\varepsilon,3}$ to these sets, we get the following images:

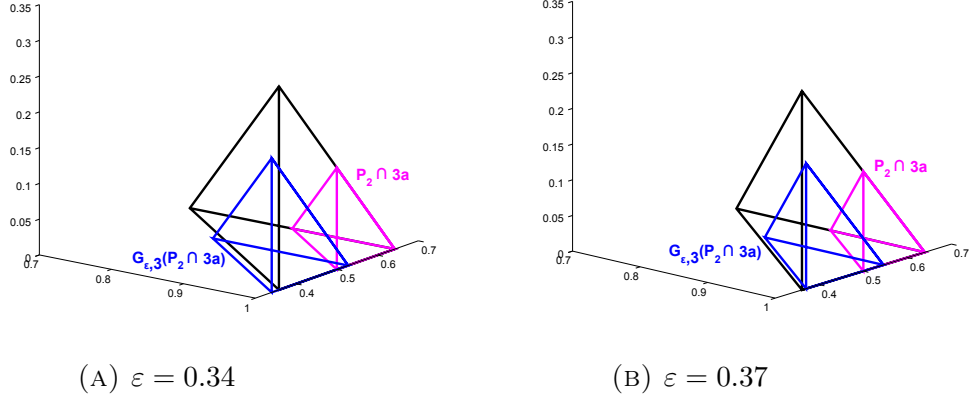


FIGURE 14. The image of $P_2 \cap 3a$ for $\varepsilon = 0.34 < \frac{1}{8}(7 - \sqrt{17})$ and $\varepsilon = 0.37 > \frac{1}{8}(7 - \sqrt{17})$.

	$\mathbf{G}_{\varepsilon,3}(\mathbf{P}_2 \cap 3a)$	$\mathbf{G}_{\varepsilon,3}(\mathbf{P}_2 \cap 3b)$	$\mathbf{G}_{\varepsilon,3}(\mathbf{P}_2 \cap 3c)$
p	$p < 1$		
q		$q > \varepsilon/2$	$q > \varepsilon/2$
r	$r > 0$		$r > 0$
p + q	$p + q > 2 - p^* - \varepsilon/2$	$p + q < 1$	$p + q > 1 - p^*$
q + r	$q + r < p^* + \varepsilon/2$	$q + r > 1$	$q + r < p^*$
p + q + r		$p + q + r < 2 - \varepsilon/2$	$p + q + r > 2 + \varepsilon/2$

	$\mathbf{G}_{\varepsilon,3}(\mathbf{P}_2 \cap 4a)$	$\mathbf{G}_{\varepsilon,3}(\mathbf{P}_2 \cap 4b)$	$\mathbf{G}_{\varepsilon,3}(\mathbf{P}_2 \cap 4c)$
p	$p < 1$		$p < 1$
q		$q < 1 - \varepsilon/2$	$q < 1 - \varepsilon/2$
r	$r > 0$		
p + q	$p + q > 2 - p^* - \varepsilon/2$	$p + q > 2 - p^* - \varepsilon/2$	$p + q > 2 - p^*$
q + r	$q + r < 1 - \varepsilon$	$q + r > 1$	$q + r < 1 + p^*$
p + q + r		$p + q + r < 2 - \varepsilon/2$	$p + q + r > 2 + \varepsilon/2$

We first notice that $G_{\varepsilon,3}(P_2 \cap 3a) \subset P_2$, if $p + q > 1 + p^*$ for the points of $G_{\varepsilon,3}(P_2 \cap 3a)$ (since $q + r < p^* + \varepsilon/2 < 1 - p^*$ for every $\varepsilon < 1/2$). This holds, if

$$1 + \varepsilon \geq 1 + p^*$$

$$\varepsilon \geq \frac{1}{8}(7 - \sqrt{17}) \approx 0.359$$

Note that $\frac{1}{8}(7 - \sqrt{17}) < \varepsilon^*$. For an illustration, see Figure 14.

We are going to describe $S_3(P_1)$, $S_4(P_1)$ and $S_3S_4(P_1)$, since we are going to need them explicitly in the upcoming calculations.

	$\mathbf{S}_3(\mathbf{P}_1)$	$\mathbf{S}_4(\mathbf{P}_1)$	$\mathbf{S}_3\mathbf{S}_4(\mathbf{P}_1)$
p	$p > 1 - p^*$	$p > 1 - p^*$	$p < 1$
q	$q > \varepsilon/2$	$q < 1 - \varepsilon/2$	$q < 1 - \varepsilon/2$
r	$r < p^*$	$r < p^*$	
p + q	$p + q < 1$		$p + q > 2 - p^*$
q + r		$q + r > 1$	$q + r < 1 + p^*$
p + q + r	$p + q + r > 1 + \varepsilon/2$	$p + q + r < 2 - \varepsilon/2$	$p + q + r > 2 + \varepsilon/2$

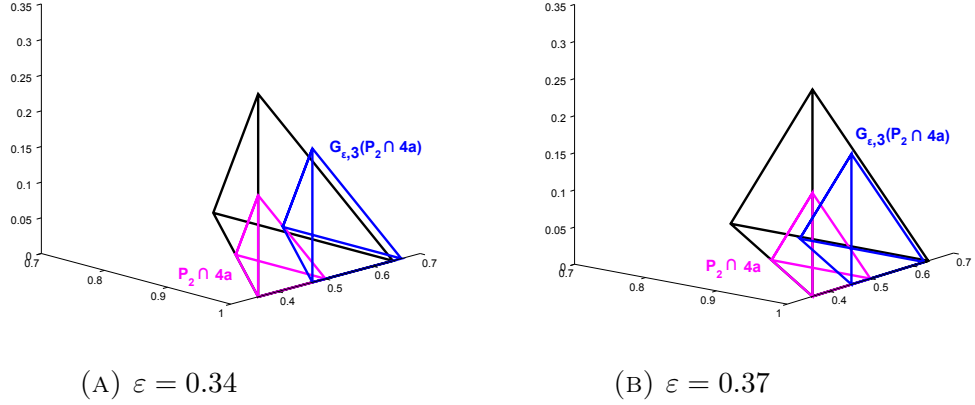


FIGURE 15. The image of $P_2 \cap 4a$ for $\varepsilon = 0.34 < \frac{1}{8}(7 - \sqrt{17})$ and $\varepsilon = 0.37 > \frac{1}{8}(7 - \sqrt{17})$.

Returning to the proof of $G_{\varepsilon,3}(P_2) \subseteq \mathcal{A}$, we claim that $G_{\varepsilon,3}(P_2 \cap 3b) \subset S_3(P_1)$. For this we have to check that $r < p^*$ and $p > 1 - p^*$ holds for the points of $G_{\varepsilon,3}(P_2 \cap 3b)$. But we see that the supremum of r on this set is exactly p^* , and the infimum of p is $1 - p^*$, so we are done.

We also see that $G_{\varepsilon,3}(P_2 \cap 3c) \subset P_1$ (the interior of these two sets actually coincide).

Moving on to $G_{\varepsilon,3}(P_2 \cap 4a)$, this set is part of P_2 , if $q + r < 1 - p^*$ holds for its points. This is the case, if

$$1 - \varepsilon \leq 1 - p^*$$

$$\frac{1}{8}(7 - \sqrt{17}) \leq \varepsilon$$

Remember that $\frac{1}{8}(7 - \sqrt{17}) < \varepsilon^*$. For an illustration, see Figure 15.

Next, we claim that $G_{\varepsilon,3}(P_2 \cap 4b) \subset S_4(P_1)$. For this we have to check that $r < p^*$ and $p > 1 - p^*$ holds for the points of $G_{\varepsilon,3}(P_2 \cap 3b)$. But we see that the supremum of r on this set is exactly p^* , and the infimum of p is $1 - p^*$, so we are done.

Finally, we see that $G_{\varepsilon,3}(P_2 \cap 4c) = S_3S_4(P_1)$.

Asymmetries of \mathcal{A} .

We first prove the asymmetry with respect to the symmetry S_0 , derived from the inversion symmetry of $F_{\varepsilon,3}$, then prove asymmetry with respect to symmetries derived from permutation symmetries of $F_{\varepsilon,3}$, namely S_1, S_2, S_5 and S_6 .

Asymmetry with respect to S_0 . Notice that is enough to check that $S_0(P_1)$ and $S_0(P_2)$ are disjoint from \mathcal{A} . This is enough indeed, since if $S_0(P_i) \subset \mathcal{A}^C$, $i = 1, 2$, then $S_0S(P_i) = SS_0(P_i) \subset S\mathcal{A}^C = \mathcal{A}^C$, if $S \subset \langle S_3, S_4 \rangle$.

In the table below, we describe $S_0(P_1), S_0(P_2)$ and $S_3(P_2) \subset \mathcal{A}$.

	$\mathbf{S}_0(\mathbf{P}_1)$	$\mathbf{S}_0(\mathbf{P}_2)$	$\mathbf{S}_3(\mathbf{P}_2)$
\mathbf{p}		$p > 0$	$p > p^*$
\mathbf{q}	$q < 1 - \varepsilon/2$		
\mathbf{r}	$r < 1$	$r < 1$	$r < 1 - p^*$
$\mathbf{p} + \mathbf{q}$	$p + q < 1 + p^*$	$p + q < 1 - p^*$	$p + q < 1$
$\mathbf{q} + \mathbf{r}$	$q + r > 2 - p^*$	$q + r > 1 + p^*$	$q + r > 1$
$\mathbf{p} + \mathbf{q} + \mathbf{r}$	$p + q + r > 2 + \varepsilon/2$		

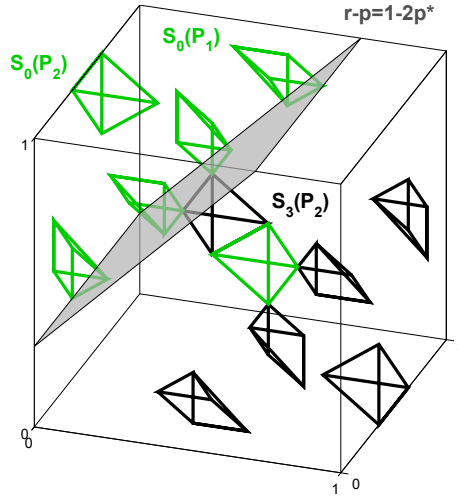


FIGURE 16. The sets \mathcal{A} (black) and $S_0(\mathcal{A})$ (green). The plane $r - p = 1 - 2p^*$ separates $S_0(P_1)$, $S_0(P_2)$ and \mathcal{A} .

We are going to show that the plane $r - p = 1 - 2p^*$ separates both $S_0(P_1)$ and $S_0(P_2)$ from \mathcal{A} . We see that the infimum of $r - p$ on $S_0(P_1)$ is exactly $1 - 2p^*$, and it is $2p^* > 1 - 2p^*$ on $S_0(P_2)$ (it is easy to see that $p^* \geq 1/3$ for every value of ε). So these sets are above the plane. On the other hand, the supremum of $r - p$ on \mathcal{A} is $1 - 2p^*$ (obtained on the closure of $S_3(P_2)$), hence this plane separates \mathcal{A} from $S_0(P_1)$ and $S_0(P_2)$. For an illustration see Figure 16.

Asymmetry with respect to S_1, S_2, S_5 and S_6 . First notice that it is enough to prove that $S_1(\mathcal{A}) \subset \mathcal{A}^C$. From this it follows that

$$\begin{aligned} S_5(\mathcal{A}) &= S_3 S_1(\mathcal{A}) \subset S_3 \mathcal{A}^C = \mathcal{A}^C, \\ S_2(\mathcal{A}) &= S_4 S_1(\mathcal{A}) \subset S_4 \mathcal{A}^C = \mathcal{A}^C, \\ S_6(\mathcal{A}) &= S_3 S_4 S_1(\mathcal{A}) \subset S_3 S_4 \mathcal{A}^C = \mathcal{A}^C. \end{aligned}$$

We now describe the six polyhedra of $S_1(\mathcal{A})$.

	$\mathbf{S}_1(\mathbf{P}_1)$	$\mathbf{S}_1(\mathbf{P}_2)$	$\mathbf{S}_1\mathbf{S}_3(\mathbf{P}_1)$
\mathbf{p}		$p > 0$	$p < p^*$
\mathbf{q}	$q > 1 - p^*$	$q > p^*$	$q < 1$
\mathbf{r}	$r > 0$	$r > 0$	$r < p^*$
$\mathbf{p} + \mathbf{q}$	$p + q > 1 + \varepsilon/2$		$p + q > 1 - \varepsilon/2$
$\mathbf{q} + \mathbf{r}$	$q + r < 1 - \varepsilon/2$		$q + r > \varepsilon/2$
$\mathbf{p} + \mathbf{q} + \mathbf{r}$	$p + q + r < 1 + p^*$	$p + q + r < 1 - p^*$	

	$\mathbf{S}_1\mathbf{S}_4(\mathbf{P}_1)$	$\mathbf{S}_1\mathbf{S}_3(\mathbf{P}_2)$	$\mathbf{S}_1\mathbf{S}_3\mathbf{S}_4(\mathbf{P}_1)$
\mathbf{p}	$p < p^*$	$p < 1 - p^*$	$p > 0$
\mathbf{q}		$q < 1$	$q > 1 - p^*$
\mathbf{r}	$r < p^*$	$r < 1 - p^*$	
$\mathbf{p} + \mathbf{q}$	$p + q < 1 - \varepsilon/2$		$p + q < 1 - \varepsilon/2$
$\mathbf{q} + \mathbf{r}$	$q + r < 1 - \varepsilon/2$		$q + r > 1 - \varepsilon/2$
$\mathbf{p} + \mathbf{q} + \mathbf{r}$	$p + q + r > 1$	$p + q + r > 2$	$p + q + r < 1 + p^*$

We first show that the plane $p + q + r = 1 - p^*$ separates $S_1(P_2)$ and \mathcal{A} . This is a consequence of the fact that the infimum of $p + q + r$ is $1 - p^*$ on \mathcal{A} (attained on the closure of P_1), and the supremum of $p + q + r$ on $S_1(P_2)$ is $1 - p^*$ (attained on the closure).

Our second observation is that the plane $q + r = 1 + p^*$ separates $S_1S_3(P_2)$ and \mathcal{A} . This holds, since the supremum of $q + r$ is $1 + p^*$ on \mathcal{A} (attained on the closure of $S_3S_4(P_1)$), and the infimum of $q + r$ on $S_1S_3(P_2)$ is $1 + p^*$ (attained on the closure).

For an illustration, see Figure 17.

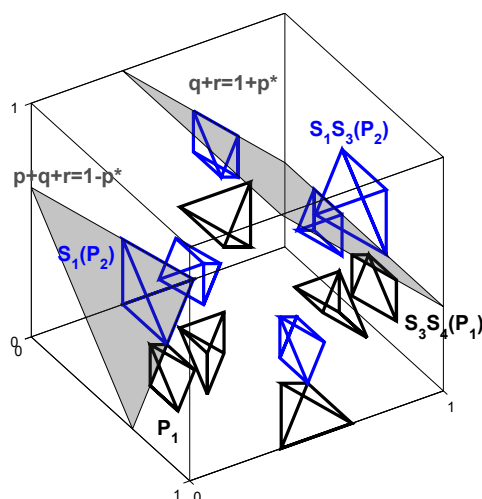
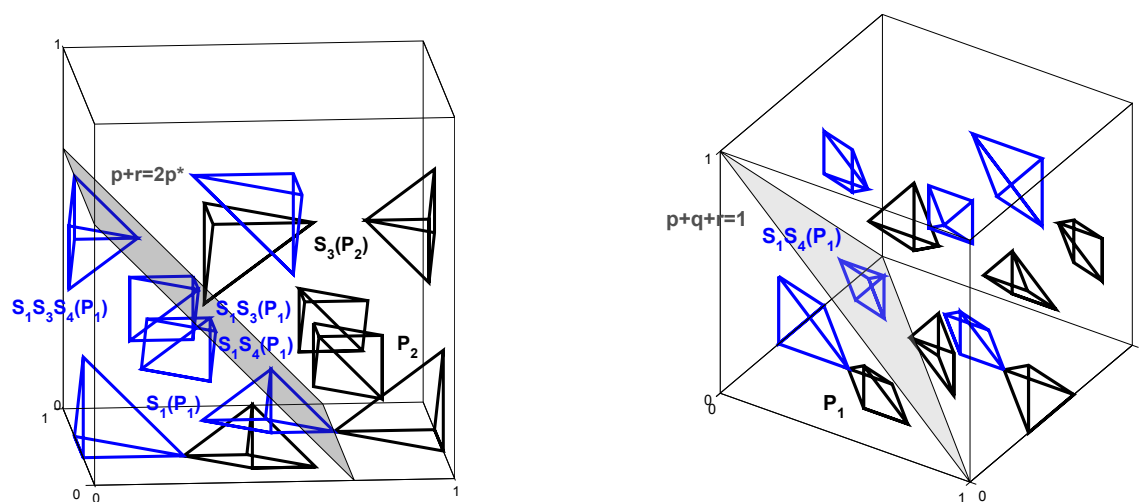


FIGURE 17. The plane $p + q + r = 1 - p^*$ separates $S_1(P_2)$ from \mathcal{A} and the plane $q + r = 1 + p^*$ separates $S_1S_3(P_2)$ from \mathcal{A} .



(A) The plane $p + r = 2p^*$ separates $S_1(P_1)$, $S_1S_3(P_1)$, $S_1S_4(P_1)$ and $S_1S_3S_4(P_1)$ from $\mathcal{A} \setminus P_1$.

(B) The plane $p + q + r = 1$ separates $S_1(P_1)$, $S_1S_3(P_1)$, $S_1S_4(P_1)$ and $S_1S_3S_4(P_1)$ from P_1 .

FIGURE 18. The sets \mathcal{A} (black) and $S_1(\mathcal{A})$ (blue).

Moving on to symmetric images of P_1 , we first claim that the plane $p+r = 2p^*$ separates $S_1(P_1)$, $S_1S_3(P_1)$, $S_1S_4(P_1)$ and $S_1S_3S_4(P_1)$ from $\mathcal{A}\setminus P_1$. This is true because the infimum of $p+r$ is $2p^*$ on $\mathcal{A}\setminus P_1$ (attained on the closure of P_2 and $S_3(P_2)$), and the supremum of $p+r$ on $S_1(P_1) \cup S_1S_3(P_1) \cup S_1S_4(P_1) \cup S_1S_3S_4(P_1)$ is $1+p^*$ (attained on the closure of all four polyhedra). For an illustration, see Figure 18a. Lastly, we claim that the plane $p+q+r = 1$ separates $S_1(P_1) \cup S_1S_3(P_1) \cup S_1S_4(P_1) \cup S_1S_3S_4(P_1)$ from P_1 . This holds because the supremum of $p+q+r$ is $1-\varepsilon/2$ on P_1 (attained on the closure), and the infimum of $p+q+r$ on $S_1(P_1) \cup S_1S_3(P_1) \cup S_1S_4(P_1) \cup S_1S_3S_4(P_1)$ is 1 (attained on the closure of $S_1S_4(P_1)$). For an illustration, see Figure 18b.

APPENDIX C: PROOF OF PROPOSITION 2

To check the symmetry properties, many straightforward calculations are needed (it suffices to check that the set \mathcal{S} is symmetric with respect to the minimal generating symmetries S_0, S_1, S_2 and S_3). We omit these calculations, since they do not bear any interesting details.

We now prove that $G_{\varepsilon,3}(\mathcal{S}) \subseteq \mathcal{S}$. To obtain this, it is enough to check that

$$G_{\varepsilon,3}(P_0) \subseteq \mathcal{S},$$

by similar arguments used to show that the invariance of \mathcal{A} was a consequence of $G_{\varepsilon,3}(P_i) \subseteq \mathcal{A}$, $i = 1, 2$.

First of all, we are going to describe the 12 polyhedra of \mathcal{S} in a table below. We will give a description with inequalities which is always correct in \mathbb{R}^3 and correct in \mathbb{T}^3 , if $1 - \frac{\sqrt{2}}{2} \leq \varepsilon$.

	P₀	S₀(P₀)
p	$L_\varepsilon(\varepsilon/2) < p < L_\varepsilon(1 - \varepsilon/2)$	$L(\varepsilon/2) < p < L_\varepsilon(1 - \varepsilon/2)$
q	$\varepsilon/2 < q < L_\varepsilon^2(1 - \varepsilon/2)$	$L_\varepsilon^2(\varepsilon/2) < q < 1 - \varepsilon/2$
r	$L_\varepsilon(\varepsilon/2) < r < L_\varepsilon(1 - \varepsilon/2)$	$L_\varepsilon(\varepsilon/2) < r < L_\varepsilon(1 - \varepsilon/2)$
p + q		
q + r		
p + q + r	$1 + \varepsilon/2 < p + q + r < 1 + L_\varepsilon^2(1 - \varepsilon/2)$	$1 + L_\varepsilon^2(\varepsilon/2) < p + q + r < 2 - \varepsilon/2$
	S₁(P₀)	S₂(P₀)
p	$L_\varepsilon(\varepsilon/2) < p < L_\varepsilon(1 - \varepsilon/2)$	$L_\varepsilon^2(\varepsilon/2) < p < 1 - \varepsilon/2$
q		$L_\varepsilon(\varepsilon/2) < q < L_\varepsilon(1 - \varepsilon/2)$
r	$L_\varepsilon(\varepsilon/2) < r < L_\varepsilon(1 - \varepsilon/2)$	$\varepsilon/2 < r < L_\varepsilon^2(1 - \varepsilon/2)$
p + q	$1 + \varepsilon/2 < p + q < 1 + L_\varepsilon^2(1 - \varepsilon/2)$	
q + r	$1 + \varepsilon/2 < q + r < 1 + L_\varepsilon^2(1 - \varepsilon/2)$	
p + q + r		$1 + L_\varepsilon(\varepsilon/2) < p + q + r < 1 + L_\varepsilon(1 - \varepsilon/2)$
	S₃(P₀)	S₄(P₀)
p		
q	$\varepsilon/2 < q < L_\varepsilon^2(1 - \varepsilon/2)$	$\varepsilon/2 < q < L_\varepsilon^2(1 - \varepsilon/2)$
r		
p + q	$L_\varepsilon(\varepsilon/2) < p + q < L_\varepsilon(1 - \varepsilon/2)$	$1 + L_\varepsilon(\varepsilon/2) < p + q < 1 + L_\varepsilon(1 - \varepsilon/2)$
q + r	$L_\varepsilon(\varepsilon/2) < q + r < L_\varepsilon(1 - \varepsilon/2)$	$1 + L_\varepsilon(\varepsilon/2) < q + r < 1 + L_\varepsilon(1 - \varepsilon/2)$
p + q + r	$L_\varepsilon^2(\varepsilon/2) < p + q + r < 1 - \varepsilon/2$	$2 + \varepsilon/2 < p + q + r < 2 + L_\varepsilon^2(1 - \varepsilon/2)$

	$\mathbf{S}_5(\mathbf{P}_0)$	$\mathbf{S}_0\mathbf{S}_1(\mathbf{P}_0)$
\mathbf{p}	$\varepsilon/2 < p < L_\varepsilon^2(1 - \varepsilon/2)$	$L_\varepsilon(\varepsilon/2) < p < L_\varepsilon(1 - \varepsilon/2)$
\mathbf{q}	$L_\varepsilon(\varepsilon/2) < q < L_\varepsilon(1 - \varepsilon/2)$	
\mathbf{r}	$L_\varepsilon^2(\varepsilon/2) < r < 1 - \varepsilon/2$	$L_\varepsilon(\varepsilon/2) < r < L_\varepsilon(1 - \varepsilon/2)$
$\mathbf{p} + \mathbf{q}$		$L_\varepsilon^2(\varepsilon/2) < p + q < 1 - \varepsilon/2$
$\mathbf{q} + \mathbf{r}$		$L_\varepsilon^2(\varepsilon/2) < q + r < 1 - \varepsilon/2$
$\mathbf{p} + \mathbf{q} + \mathbf{r}$	$1 + L_\varepsilon(\varepsilon/2) < p + q + r < 1 + L_\varepsilon(1 - \varepsilon/2)$	

	$\mathbf{S}_2\mathbf{S}_1(\mathbf{P}_0)$	$\mathbf{S}_3\mathbf{S}_1(\mathbf{P}_0)$
\mathbf{p}		$L_\varepsilon^2(\varepsilon/2) < p < 1 - \varepsilon/2$
\mathbf{q}	$L_\varepsilon(\varepsilon/2) < q < L_\varepsilon(1 - \varepsilon/2)$	
\mathbf{r}		$L_\varepsilon^2(\varepsilon/2) < r < 1 - \varepsilon/2$
$\mathbf{p} + \mathbf{q}$	$L_\varepsilon^2(\varepsilon/2) < p + q < 1 - \varepsilon/2$	$1 + L_\varepsilon(\varepsilon/2) < p + q < 1 + L_\varepsilon(1 - \varepsilon/2)$
$\mathbf{q} + \mathbf{r}$	$1 + \varepsilon/2 < q + r < 1 + L_\varepsilon^2(1 - \varepsilon/2)$	$1 + L_\varepsilon(\varepsilon/2) < q + r < 1 + L_\varepsilon(1 - \varepsilon/2)$
$\mathbf{p} + \mathbf{q} + \mathbf{r}$	$1 + L_\varepsilon(\varepsilon/2) < p + q + r < 1 + L_\varepsilon(1 - \varepsilon/2)$	

	$\mathbf{S}_4\mathbf{S}_1(\mathbf{P}_0)$	$\mathbf{S}_5\mathbf{S}_1(\mathbf{P}_0)$
\mathbf{p}	$\varepsilon/2 < p < L_\varepsilon^2(1 - \varepsilon/2)$	
\mathbf{q}		$L_\varepsilon(\varepsilon/2) < q < L_\varepsilon(1 - \varepsilon/2)$
\mathbf{r}	$\varepsilon/2 < r < L_\varepsilon^2(1 - \varepsilon/2)$	
$\mathbf{p} + \mathbf{q}$	$L_\varepsilon(\varepsilon/2) < p + q < L_\varepsilon(1 - \varepsilon/2)$	$1 + \varepsilon/2 < p + q < 1 + L_\varepsilon^2(1 - \varepsilon/2)$
$\mathbf{q} + \mathbf{r}$	$L_\varepsilon(\varepsilon/2) < q + r < L_\varepsilon(1 - \varepsilon/2)$	$L_\varepsilon^2(\varepsilon/2) < q + r < 1 - \varepsilon/2$
$\mathbf{p} + \mathbf{q} + \mathbf{r}$		$1 + L_\varepsilon(\varepsilon/2) < p + q + r < 1 + L_\varepsilon(1 - \varepsilon/2)$

Observe that the polyhedron P_0 intersects four domains of continuity, 1e, 4b, 5b and 8b in the following way:

	$\mathbf{P}_0 \cap 1\mathbf{e}$	$\mathbf{P}_0 \cap 4\mathbf{b}$
\mathbf{p}	$L_\varepsilon(\varepsilon/2) < p < 1/2$	$1/2 < p < L_\varepsilon(1 - \varepsilon/2)$
\mathbf{q}	$\varepsilon/2 < q < L_\varepsilon^2(1 - \varepsilon/2)$	$\varepsilon/2 < q < L_\varepsilon^2(1 - \varepsilon/2)$
\mathbf{r}	$L_\varepsilon(\varepsilon/2) < r < 1/2$	$L_\varepsilon(\varepsilon/2) < r < 1/2$
$\mathbf{p} + \mathbf{q} + \mathbf{r}$	$1 + \varepsilon/2 < p + q + r < 1 + L_\varepsilon^2(1 - \varepsilon/2)$	$1 + \varepsilon/2 < p + q + r < 1 + L_\varepsilon^2(1 - \varepsilon/2)$

	$\mathbf{P}_0 \cap 5\mathbf{b}$	$\mathbf{P}_0 \cap 8\mathbf{b}$
\mathbf{p}	$L_\varepsilon(\varepsilon/2) < p < 1/2$	$1/2 < p < L_\varepsilon(1 - \varepsilon/2)$
\mathbf{q}	$\varepsilon/2 < q < L_\varepsilon^2(1 - \varepsilon/2)$	$\varepsilon/2 < q < L_\varepsilon^2(1 - \varepsilon/2)$
\mathbf{r}	$1/2 < r < L_\varepsilon(1 - \varepsilon/2)$	$1/2 < r < L_\varepsilon(1 - \varepsilon/2)$
$\mathbf{p} + \mathbf{q} + \mathbf{r}$	$1 + \varepsilon/2 < p + q + r < 1 + L_\varepsilon^2(1 - \varepsilon/2)$	$1 + \varepsilon/2 < p + q + r < 1 + L_\varepsilon^2(1 - \varepsilon/2)$

We calculate the images of these polyhedra, using that the coordinates p, q and r evolve according to L_ε in domains 4b and 5b and the coordinates p and r evolve according to L_ε in domains 1e and 8b. The results are collected in the table below.

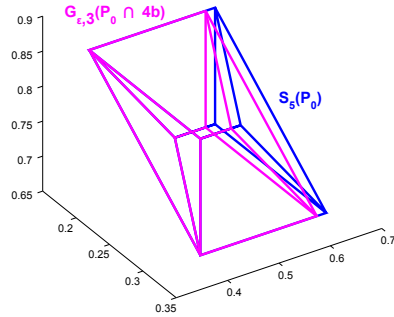
	$\mathbf{G}_{\varepsilon,3}(\mathbf{P}_0 \cap 1\mathbf{e})$	$\mathbf{G}_{\varepsilon,3}(\mathbf{P}_0 \cap 4\mathbf{b})$
\mathbf{p}	$L_\varepsilon^2(\varepsilon/2) < p < 1 - \varepsilon/2$	$\varepsilon/2 < p < L_\varepsilon^2(1 - \varepsilon/2)$
\mathbf{q}	$L_\varepsilon(\varepsilon/2) + \varepsilon/2 < q < L_\varepsilon^3(1 - \varepsilon/2) + \varepsilon/2$	$L_\varepsilon(\varepsilon/2) < q < L_\varepsilon^3(1 - \varepsilon/2)$
\mathbf{r}	$L_\varepsilon^2(\varepsilon/2) < r < 1 - \varepsilon/2$	$L_\varepsilon^2(\varepsilon/2) < r < 1 - \varepsilon/2$
$\mathbf{p} + \mathbf{q} + \mathbf{r}$	$1 + L_\varepsilon(\varepsilon/2) + \varepsilon/2 < p + q + r < 1 + L_\varepsilon^3(1 - \varepsilon/2) + \varepsilon/2$	$1 + L_\varepsilon(\varepsilon/2) < p + q + r < 1 + L_\varepsilon^3(1 - \varepsilon/2)$

	$\mathbf{G}_{\varepsilon,3}(\mathbf{P}_0 \cap 5b)$	$\mathbf{G}_{\varepsilon,3}(\mathbf{P}_0 \cap 8b)$
\mathbf{p}	$L_\varepsilon^2(\varepsilon/2) < p < 1 - \varepsilon/2$	$\varepsilon/2 < p < L_\varepsilon^2(1 - \varepsilon/2)$
\mathbf{q}	$L_\varepsilon(\varepsilon/2) < q < L_\varepsilon^3(1 - \varepsilon/2)$	$L_\varepsilon(\varepsilon/2) - \varepsilon/2 < q < L_\varepsilon^3(1 - \varepsilon/2) - \varepsilon/2$
\mathbf{r}	$\varepsilon/2 < r < L_\varepsilon^2(1 - \varepsilon/2)$	$\varepsilon/2 < r < L_\varepsilon^2(1 - \varepsilon/2)$
$\mathbf{p} + \mathbf{q} + \mathbf{r}$	$1 + L_\varepsilon(\varepsilon/2) < p + q + r < 1 + L_\varepsilon^3(1 - \varepsilon/2)$	$1 + L_\varepsilon(\varepsilon/2) - \varepsilon/2 < p + q + r < 1 + L_\varepsilon^3(1 - \varepsilon/2) - \varepsilon/2$

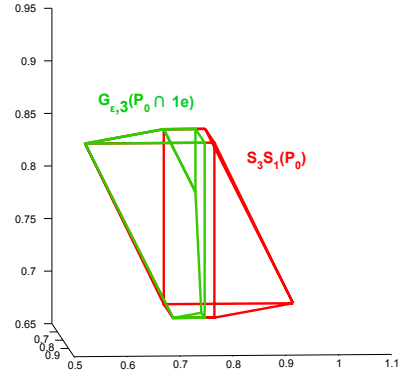
We immediately see that $G_{\varepsilon,3}(P_0 \cap 4b) \subseteq S_5(P_0)$ if and only if

$$L_\varepsilon^3(1 - \varepsilon/2) \leq L_\varepsilon(1 - \varepsilon/2)$$

$$1 - \frac{\sqrt{2}}{2} \leq \varepsilon.$$



(A) The image of $P_0 \cap 4b$. The case of the image of $P_0 \cap 5b$ is geometrically very similar.



(B) The image of $P_0 \cap 1e$. The case of the image of $P_0 \cap 8b$ is geometrically very similar.

FIGURE 19. Images of $P_0 \cap 4b$ and $P_0 \cap 1e$ for $\varepsilon = 0.32 > 1 - \frac{\sqrt{2}}{2}$.

We also see that $G_{\varepsilon,3}(P_0 \cap 5b) \subseteq S_2(P_0)$ if and only if

$$L_\varepsilon^3(1 - \varepsilon/2) \leq L_\varepsilon(1 - \varepsilon/2)$$

$$1 - \frac{\sqrt{2}}{2} \leq \varepsilon.$$

For an illustration, see Figure 19a.

Now let us turn to $G_{\varepsilon,3}(P_0 \cap 1e)$. The infimum of $p+q$ on this polyhedron is $1 + L_\varepsilon(\varepsilon/2)$ and the supremum is $1 + L_\varepsilon^3(1 - \varepsilon/2)$. The same holds for $q+r$. So we see that $G_{\varepsilon,3}(P_0 \cap 1e) \subseteq S_3S_1(P_0)$ if and only if

$$L_\varepsilon^3(1 - \varepsilon/2) \leq L_\varepsilon(1 - \varepsilon/2)$$

$$1 - \frac{\sqrt{2}}{2} \leq \varepsilon.$$

Finally, moving on to $G_{\varepsilon,3}(P_0 \cap 8b)$. The infimum of $p + q$ on this polyhedron is $L_\varepsilon(\varepsilon/2)$ and the supremum is $L_\varepsilon^3(1 - \varepsilon/2)$. The same holds for $q + r$. So we see that $G_{\varepsilon,3}(P_0 \cap 8b) \subseteq S_4 S_1(P_0)$ if and only if

$$\begin{aligned} L_\varepsilon^3(1 - \varepsilon/2) &\leq L_\varepsilon(1 - \varepsilon/2) \\ 1 - \frac{\sqrt{2}}{2} &\leq \varepsilon. \end{aligned}$$

For an illustration, see Figure 19b.

E-mail address: selley@math.bme.hu